NAMT

qa-oas

Energy Minimization and the Formation of Microstructure in Dynamic Anti-Plane Shear

Pieter J. Swart
Department of Mathematics
Carnegie Mellon University
Pittsburgh, PA 15213-3890

and

Philip J. Holmes
Department of Theoretical and Applied Mechanics and
Center for Applied Mathematics
Cornell University
Ithaca, NY 14853

Research Report No. 92-NA-025

August 1992

Energy Minimization and the Formation of Microstructure in Dynamic Anti-Plane Shear

PIETER J. SWART & PHILIP J. HOLMES

Abstract

We investigate the behavior of a continuum model designed to provide insight into the dynamical development of microstructures observed during displacive phase transformations in certain materials. The model is presented within the framework of nonlinear viscoelasticity and is also of interest as an example of a strongly dissipative infinite–dimensional dynamical system whose forward orbits need not lie on a finite–dimensional attracting set, and which can display a subtle dependence on initial conditions quite different from that of classical finite dimensional "chaos".

We study the problem of dynamical (two–dimensional) anti–plane shear with linear viscoelastic damping. Within the framework of nonlinear hyperelasticity, we consider both isotropic and anisotropic constitutive laws which can allow different phases and we characterize their ability to deliver minimizers and minimizing sequences of the stored elastic energy (Theorem 2.3) Using a transformation due to RYBKA, the problem is recast as a semilinear degenerate parabolic system, thereby allowing the application of semigroup theory to establish existence, uniqueness and regularity of solutions in L^p spaces (Theorem 3.1). We also discuss the issues of energy minimization and propagation of strain discontinuities. We comment on the difficulties encountered in trying to exploit the geometrical properties of specific constitutive laws. In particular we are unable to obtain analogues of the failure to minimize and non–propagation of strain discontinuity results obtained by BALL, HOLMES, JAMES, PEGO & SWART [1991] for a one–dimensional model problem.

Several numerical experiments are presented, which prompt the following conclusions. It appears that the absence of an absolute minimizer may prevent energy minimization, thereby providing a dynamical mechanism to limit the fineness of observed microstructure, as has been proven in the one–dimensional case. Similarly, viscoelastic damping appears to prevent the propagation of strain discontinuities. During the extremely slow development of fine structure, solutions are observed to display local refinement in an effort to overcome incompatibility at the boundary and with initial conditions, with the distribution and shape of the resulting finer scales displaying a subtle dependence on initial conditions.

Contents

1 Introduction

For many dissipative physical processes it is assumed that observable equilibrium states correspond to the minima of some underlying energy function. The first clear enunciation of such a principle is perhaps that of GIBBS [1876]:

> *For the equilibrium of any isolated system it is necessary and sufficient that in all possible variations of the state of the system which do not alter its entropy, the variation of its energy shall either vanish or be positive.*

In interpreting such statements physically, the question of how a system approaches an equilibrium from an arbitrary initial state is of great importance. It is, for example, of concern to know how rapidly such states are achieved, and if they are achieved by all solutions, merely a subset, or possibly none at all.

For physical models based on ordinary differential equations possessing Liapunov functions, the theory is well–developed (cf. LASALLE & LEFSCHETZ [1961]) — all solutions converge to critical points of the underlying energy and almost all solutions converge to local minima. However, for models such as those provided by the partial differential equations

of continuum mechanics, including those under consideration in this paper, the situation can be much more complex (cf. BALL [1990], HALE [1988]). Nonetheless, the dogma of energy minimization exemplified by GIBB's statement has dominated thinking to the extent that much of the analysis of continuum problems amounts to a search for equilibrium solutions which are minimizers of some type.

The past two decades have witnessed the development of various physical theories based on variational formulations that require the minimization of an "energy" which suffers a severe loss in convexity. The most outstanding example, and the one of concern in this work, is the use of nonconvex stored energy functions to model displacive phase transformations — solid–solid phase transformations which are accompanied by a change of shape — in certain ionic solids, shape memory alloys and ferro–electrics. Within the elasticity literature, this approach has its origins in the work of ERICKSEN [1975], [1980], KNOWLES & STERNBERG [1975], [1977], [1978], and JAMES [1979], [1980]. Not only has it yielded significant new insights and accurate quantitative descriptions of experimentally observed phenomena, but it has also been responsible for a resurgence of interest and subsequent research in variational methods and their applications to partial differential equations.

Against this background, BALL, HOLMES, JAMES, PEGO & SWART [1991] studied some one–dimensional model problems from a dynamical perspective, the most relevant to the present paper representing a non–convex viscoelastic continuum bonded by linear "glue" to a rigid substrate. We briefly review their results at the end of §2.1. The remainder of this work is devoted to the dynamical anti–plane shear problem with viscoelastic damping. We discuss both the isotropic and anisotropic cases, with the emphasis on anisotropic constitutive laws which allow several different phases. This problem is defined in §2, where the issues of existence, uniqueness and stability of solutions are also discussed. Theorem 2.3 characterizes the ability of constitutive laws to deliver minimizing sequences and classical minimizers. Theorem 3.1 gives global existence and uniqueness, albeit under physically

restrictive assumptions, and the difficulties of relaxing these assumptions are discussed. We are, unfortunately, unable to obtain analogues of the nonminimization and strain discontinuity persistence results of the one–dimensional models of BALL et al. [1991], and in §4 we discuss some reasons for this. In §5 we describe a finite difference scheme and in §6 we present the results of numerical experiments. We display the dynamical evolution of microstructure and show numerical evidence for the persistence of strain discontinuities and subtle dependence on initial conditions, as well as an example of apparent non–minimization of the energy. Conclusions and suggestions for possible extensions are contained in §7.

Throughout, Ω will denote an open and bounded set in R^n with a Lipschitz smooth boundary $\partial\Omega$. For $1 \le p < \infty$, $L^p(\Omega, \mathrm{R}^m)$ is the Banach space of measurable functions $\mathbf{u} : \Omega \to \mathrm{R}^m$ for which

$$\|\mathbf{u}\|_{L^p} = (\int_\Omega |\mathbf{u}(\mathbf{x})|^p \, \mathbf{dx})^{\frac{1}{p}} < \infty;$$

we write $L^p(\Omega)$ if $m = 1$ and L^p if the domain and the range are understood. We use a bold font to indicate that a variable or operator is vector– or tensor–valued. We let $\|\mathbf{u}\| \equiv \|\mathbf{u}\|_{L^2}$ and $(\mathbf{u}, \mathbf{v}) \equiv \int_\Omega \mathbf{u} \cdot \overline{\mathbf{v}} \, \mathbf{dx}$ denote the L^2 norm and inner product of the (complex valued) functions $\mathbf{u}, \mathbf{v} \in L^2$ (overbars denote complex conjugates). For $p = \infty$, $L^\infty(\Omega, \mathrm{R}^m)$ is the space of measurable and essentially bounded functions $\mathbf{u}$ equipped with the norm

$$\|\mathbf{u}\|_\infty \equiv \|\mathbf{u}\|_{L^\infty} = \operatorname{ess\,sup}_{x \in \Omega} |\mathbf{u}(\mathbf{x})|.$$

For $k = 0, 1, 2, \ldots$ and $1 \le p \le \infty$, the Sobolev space $W^{k,p}(\Omega, \mathrm{R}^m)$ is the space of functions $\mathbf{u}$ in $L^p(\Omega, \mathrm{R}^m)$ whose distributional derivatives of order $\le k$ are in $L^p(\Omega)$; this is a Banach space with norm

$$\|\mathbf{u}\|_{W^{k,p}(\Omega)} = \sum_{|\alpha| \le k} \|D^\alpha \mathbf{u}\|_{L^p(\Omega)}.$$

For $p = 2$ we will write $H^k(\Omega) \equiv W^{k,2}(\Omega)$ with $\|\mathbf{u}\|_k \equiv \|\mathbf{u}\|_{H^k(\Omega)}$ and $(\mathbf{u}, \mathbf{v})_k = \sum_{|\alpha| \le k} (D^\alpha u, D^\alpha v)$. $C_0^\infty(\Omega)$ is the space of infinitely smooth test functions having compact support and $W_0^{k,p}(\Omega)$

denotes the completion of $C_0^\infty(\Omega)$ with respect to the $W^{k,p}$ norm. Any $u \in W^{k,p}(Q)$ is determined only up to a set of measure zero and we will call such a u continuous, bounded, etc. if there is a function $\tilde{u}$ with these properties and $\tilde{u} = u$ a.e. For a function $u : S \to X$ mapping an open subset S of a Banach space to another Banach space X, we write $u \in L(S, X)$ if u is a linear and bounded operator, and write $u \in C^{k,\alpha}(S, X)$ (for $k = 0, 1, 2, \ldots$ and $0 \leq \alpha \leq 1$) if $u \in C^k$ and if all the k-th order derivatives of u are Hölder continuous with Hölder exponent a. The norm is

$$\|u\|_{C^{k,\alpha}(S,X)} = \sum_{j=0}^{k} \sup_{S} \|D^j u\| + \sup_{x \neq y} \frac{\|D^k u(x) - D^k u(y)\|}{\|x - y\|^\alpha}.$$

The last term is omitted if $\alpha = 0$ and we will write $C^k \equiv C^{k,0}$ and $C \equiv C^0$. For more details see for example ADAMS [1975].

2 A Dynamical Anti-Plane Shear Problem

2.1 Continuum Modeling of Displacive Phase Transformations

Consider a homogeneous solid body occupying a region $\Omega \subset \mathbb{R}^n$ in the reference configuration (with unit density) and subject to a deformation $u : \Omega \to \mathbb{R}^n$. We are interested in modeling solid-solid phase transformations that lead to the coexistence of several different phases, and do so by supposing that, for energetic reasons, the body prefers to be (locally) deformed in one of a possibly finite number of different phases, each specified by a constant deformation gradient $F = \nabla u$. In the spirit of GIBBS, we can therefore view an equilibrium state of the body as a minimizer of the bulk energy

$$J(u) = \int_{\Omega} W(\nabla u)\, dx \tag{2.1}$$

on some admissible set of functions determined by boundary conditions, body forces, etc. Here W is the Gibbs free energy per unit reference volume, and we will assume henceforth

that it depends only on the deformation gradient, and that thermal effects, chemical composition and other determinants of material behavior can be neglected or controlled. This approach fits into the framework of nonlinear hyperelasticity, in which W is referred to as the stored elastic energy function (or strain energy density function) and the functional I is known as the total (stored) elastic energy or the total strain energy. The first Piola-Kirchoff stress tensor $\boldsymbol{\sigma}$ is then given by $\boldsymbol{\sigma}(\mathbf{F}) = \partial W/\partial \mathbf{F}$; the Fréchet derivative of the local stored energy function (cf. TRUESDELL & NOLL [1965], CIARLET [1988]). What distinguishes the models discussed here from those of conventional hyperelasticity, is that the stored energy function W is allowed to have several potential wells, thereby permitting minimizers and hence equilibrium states containing a mixture of phases with boundaries across which strain $\nabla \mathbf{u}$ may be discontinuous.

For a sufficiently smooth stored energy function W, any smooth admissible minimizer must satisfy the associated Euler–Lagrange equation

$$\mathbf{div}\boldsymbol{\sigma}(\nabla \mathbf{u}) = \mathbf{0} \text{ in } \Omega, \tag{2.2}$$

due to the vanishing of the first variation of I. In our case $W(\cdot)$ is not rank–1 convex and (2.2), augmented by suitable boundary conditions, typically admits a multitude of minimizers corresponding to complicated phase mixtures. This severe nonuniqueness is to some extent due to ignoring the dynamical process responsible for selecting a particular steady state dependent on initial data (cf. JAMES [1980]). To examine this, we will approach the minimization problem from a dynamical systems viewpoint, which also provides a (reasonably) well-developed and intuitively appealing framework for analyzing the important question of stability of equilibria (cf. HENRY [1981]).

We incorporate inertial effects by adding the kinetic energy to (2.1) to give the total energy

$$E[\mathbf{u}, \mathbf{u}_t] = \tfrac{1}{2} \int_\Omega |\mathbf{u}_t|^2 \, \mathbf{dx} + \int_\Omega W(\nabla \mathbf{u}) \, \mathbf{dx}, \tag{2.3}$$

and the corresponding equation of motion

$$\mathbf{u}_{tt} = \mathbf{div}\boldsymbol{\sigma}(\nabla \mathbf{u}) \text{ in } \Omega, \tag{2.4}$$

together with appropriate boundary conditions.

The loss of ellipticity in the stationary problem (2.2) associated with nonconvex W now corresponds to a failure of hyperbolicity in the dynamical problem (2.4). The dynamical instability associated with non–hyperbolic "phases" in problems of mixed type has excluded establishing even short–time existence of solutions to (2.4). (For W strongly elliptic, i.e. ruling out phase changes, HUGHES, KATO & MARSDEN [1977] showed the short–time existence of classical solutions in $W^{2,p}(\mathrm{R}^n, \mathrm{R}^n)$, for all $p > 1 + n/2$ — note that this result does not allow for strain discontinuities.) Moreover, the hyperbolic nature of the dynamical problem (2.4) allows discontinuities to form in finite time, necessitating the study of weak solutions that allow shock–like spatial discontinuities in the deformation gradients as well as the stress. The lack of uniqueness for these weak solutions indicates a deficiency in the constitutive modeling of moving interfaces of discontinuity. We now describe two important ways to overcome this problem, although we subsequently consider only the second.

The first approach involves constructing more detailed constitutive models that can describe the nonequilibrium thermodynamics of multi–phase materials and the evolution of the interfaces of discontinuity that they allow (cf. ABEYARATNE & KNOWLES [1990], GURTIN & STRUTHERS [1990], and the references therein). For non–convex stored energy functions W, the second law of thermodynamics in the form of the Clausius–Duhem inequality (cf. TRUESDELL & NOLL [1965]) is no longer sufficient to select a unique weak solution, necessitating additional constitutive assumptions governing the rate of entropy production. In the context of isothermal one–dimensional bars that allow phase–changes, ABEYARATNE and KNOWLES (cf. ABEYARATNE & KNOWLES [1989] and references therein to their previous work) introduced the concept of a shock–driving traction as the "force on a defect"

to account for the rate of entropy production due to a moving strain discontinuity. They then proceeded to show that a single relation controlling the kinetics of the phase transformation together with an initiation criterion is sufficient to uniquely select a weak solution for the Riemann problem. This approach was generalized to the three–dimensional theory (ABEYARATNE & KNOWLES [1990]) but at this stage still seems to preclude application to specific three–dimensional boundary value problems.

We follow a second route, namely that of regularization. The addition of linear viscoelastic damping to (2.4) to yield the quasilinear equation

$$\mathbf{u}_{tt} = \mathbf{div}(\sigma(\nabla \mathbf{u}) + \mu \nabla \mathbf{u}_t), \tag{2.5}$$

is sufficient to ensure the existence and uniqueness of strong solutions (RYBKA [1992]). This allows one to study the problem within the framework of dynamical systems theory and to analyze conditions for long–time existence, stability of equilibria, structure of the ω–limit set, etc. Another motivation for studying the regularized problem is the philosophy that a weak solution of (2.4) is admissible only if it can be obtained as a solution to the regularized equation in the limit of vanishing viscosity (and possibly also other vanishing "higher order" quantities such as capillarity, thermal conductivity, etc.) (cf. DAFERMOS [1973], SLEMROD [1989], and additional references therein). Since viscosity forces the energy to decrease, this is a physically natural method for finding (local) minima of the elastic energy (2.3). Although we expect to observe the same stationary states as may be obtained by numerical relaxation (e.g. COLLINS & LUSKIN [1989]), our approach attempts to model the dynamical process of attaining these stationary states. Thus, for a given ensemble of initial states, we expect to observe a statistically more representative picture of the material behavior. Moreover, this approach should provide insight into possible metastable states, and also allow us to study the evolution of phase boundaries.

As a first step in this direction, BALL et al. [1991] considered several one–dimensional

dynamical model problems with energies lacking absolute minimizers. In particular they were able to prove that the initial boundary value problem (BVP)

$$\begin{aligned} u_{tt} &= (u_x^3 - u_x + \mu u_{xt})_x - \alpha u\,; \quad \mu, \alpha > 0, \\ u(0,t) &= u(1,t) = 0, \\ u(x,0) &= u_0(x) \in W_0^{1,\infty}, \quad u_t(x,0) = u_1(x) \in L^2, \end{aligned} \tag{2.6}$$

possesses globally unique strong solutions. They also showed that the continuum of equilibrium solutions satisfying

$$\begin{aligned} (\tilde{u}_x^3 - \tilde{u}_x)_x - \alpha \tilde{u} &= 0, \\ \tilde{u}(0) = \tilde{u}(1) &= 0 \end{aligned} \tag{2.7}$$

and $3\tilde{u}^2 - 1 \geq \sigma_0 > 0$ a.e. are exponentially asymptotically stable to perturbations which do not move or introduce strain discontinuities. Such solutions are weak relative minimizers (JAMES [1981]) of the total energy

$$E[u, u_t] = \tfrac{1}{2}\int_0^1 u_t^2\, dx + \int_0^1 [\tfrac{1}{4}(u_x^2 - 1)^2 + \frac{\alpha}{2}u^2]\, dx. \tag{2.8}$$

PEGO [1987, Theorem 5.4] showed that an equation similar to (2.6) but with $\alpha = 0$, exhibited convergence to equilibria having discontinuous strain; moreover, he showed that, if the (smooth) initial strain data $u_{0,x}(x)$ has "near discontinuities" at $x_1, x_2, \ldots$ then these "sharpen up" and do not move much (PEGO [1987, Theorem 6.1]). When $\alpha \neq 0$ one naturally asks if the additional term in E can promote the creation of new discontinuities not present in the initial data. In particular, do "typical" solutions realize global minimizing sequences? The latter behavior is excluded by the following:

Theorem 2.1 (BALL et al. [1991], Theorem 4.1) *There is no solution of* (2.6) *which minimizes energy absolutely as* $t \to \infty$*; i.e. there is no solution such that* $E(t) \to 0$ *as* $t \to \infty$.

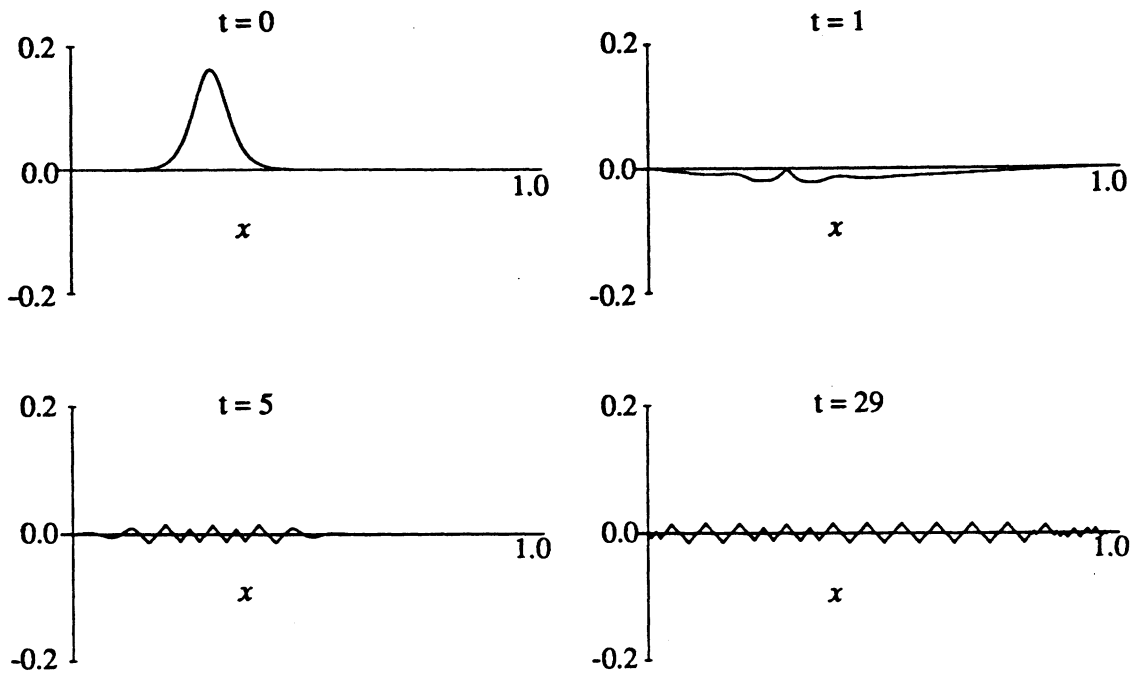

Figure 1: Numerical solution of (2.6), representing $u(x,t)$ for $0 < x < 1$; $\mu = 0.1$, $\alpha = 500$, and initial data $u_0(x) = 0.2\,\mathrm{sech}^2((x-0.3)/20)\sin \pi x$, $u_1(x) = 0$.

This result (proved by contradiction) is partially illuminated by the following, which shows that strain discontinuities cannot move, or form, or dissipate in finite time:

Theorem 2.2 (BALL et al. [1991], Theorem 4.10) *Let $\{u, u_t\}$ be a strong solution to* (2.6). *Then, if for any $t_0 \geq 0$, x_0 is a point of continuity of $u_x(t_0)$, it will remain so for all $t > t_0$. Likewise, if x_0 is a point of discontinuity of $u_x(t_0)$, it will remain so for all $t > t_0$.*

Since we work with $u \in W_0^{1,\infty}$, by a point of continuity we mean that $u_x \in L^\infty$ has a bounded representative continuous at x_0, and by a point of discontinuity, that it does not. We note that this result is not expected to hold if, for example, capillarity terms are added, since they will permit (slow) phase rearrangement.

These results suggest that typical initial data with "smooth" phase boundaries will

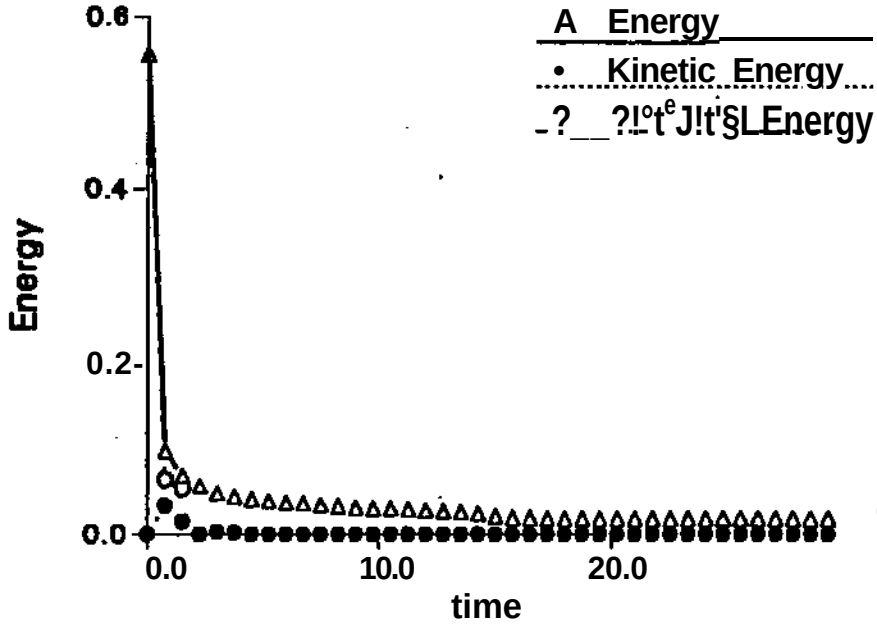

Figure 2: Energy decay for the solution of (2.6) shown in Figure 1 (a = 500).

sharpen up towards "frozen" strain discontinuities and that the creation of new boundaries will be inhibited, leading to a range of *finite* scales strongly dependent on the initial data. The resulting lack of energy minimization is nicely illustrated in Figures 1 and 2, which displays the results of numerical simulation using a one-dimensional version of the finite difference algorithm described in §5. For the computation we used a spatial mesh with $6x = 10^{-3}$ and a timestep of $St = 10^{-6}$.

The present paper represents an attempt to extend these results to multidimensional and more mechanically realistic models. We study a special class of time-dependent displacement boundary value problems associated with anti-plane shear deformations of a homogeneous, incompressible but *not necessarily isotropic* hyperelastic solid. Restricting attention to these simple deformations has the advantage of reducing the number of spatial dimensions while still allowing for interesting two-dimensional geometric effects. For this reason anti-plane shear has served as an important pilot problem in several fields (cf. KNOWLES [1976], [1977], KNOWLES & STERNBERG [1980], GURTIN & TEMAM [1981],

SILLING [1988a], [1988b], ROSAKIS [1992], FRIED [1991]).

2.2 Anti–Plane Shear

Suppose a homogeneous and incompressible hyperelastic body occupies the three–dimensional region $\Omega \times \mathrm{R} \subset \mathrm{R}^3$ in the unstressed state. The two–dimensional cross–section Ω of the region $\Omega \times \mathrm{R}$ is assumed to be a simply connected and bounded open domain in the (x, y)–plane, normal to the z–axis and with a boundary $\partial\Omega$ that is at least Lipschitz smooth. For ease of presentation, we will assume the boundary to be sufficiently smooth where so required. (However, we do remark that, with some additional effort, most of our results can be shown to require only that $\partial\Omega$ possesses no re–entrant corners.) With $\mathbf{x} = (x, y, z)$, a deformation of the form

$$\mathbf{u} : (x, y, z) \mapsto (x, y, z + u(x, y)) \tag{2.9}$$

is called an anti–plane shear with an "out–of–plane" displacement field $u : \Omega \to \mathrm{R}$. The corresponding deformation gradient $\mathbf{F} = \nabla\mathbf{u}$ has the simple form

$$\mathbf{F} = \begin{bmatrix} 1 & 0 & 0 \\ 0 & 1 & 0 \\ u_x & u_y & 1 \end{bmatrix}, \tag{2.10}$$

so that $det\,\mathbf{F} = 1$, thereby automatically satisfying the constraint of incompressibility.

We recall the equations of nonlinear elastodynamics in the absence of body forces (2.4) and with additional linear viscoelastic damping of Kelvin–Voigt type:

$$\mathbf{u}_{tt} = \mathbf{div}\boldsymbol{\tau} = \mathbf{div}(\boldsymbol{\sigma}(\nabla\mathbf{u}) + \mu\nabla\mathbf{u}_t). \tag{2.11}$$

Here μ is a positive constant specifying the size of the viscoelastic damping and we have taken the material to have unit density. We define the out–of–plane shear stress response function $\boldsymbol{\sigma} : \mathrm{R}^2 \to \mathrm{R}^2$ by

$$\boldsymbol{\sigma}(\nabla u) \equiv \boldsymbol{\sigma}((u_x, u_y)) \equiv (\sigma_{31}(\mathbf{F}), \sigma_{32}(\mathbf{F})), \tag{2.12}$$

where the deformation gradient $\mathbf{F}$ is given by (2.10) and σ_{3i} $(i = 1, 2)$ are the out–of–plane components of the Piola–Kirchoff stress $\boldsymbol{\sigma}$. The z–component of (2.11) then delivers the two–dimensional equation of motion for the out–of–plane displacement field u for anti–plane shear :

$$u_{tt} = div\boldsymbol{\sigma}(\nabla u) + \mu \Delta u_t \quad \text{in } \Omega. \tag{2.13}$$

In this work we consider the Dirichlet initial–boundary value problem with

$$u = 0 \quad \text{on } \partial\Omega, \tag{2.14}$$

and with initial data

$$u(x, y, 0) = u_0(x, y), \;\; u_t(x, y, 0) = u_1(x, y). \tag{2.15}$$

Note that (2.14) is (in principle) not a restriction, since nonzero displacement boundary conditions can be incorporated into the stress–strain response $\boldsymbol{\sigma}$.

We remark that the question of whether a specific three–dimensional constitutive law can sustain anti–plane shear is not trivial (cf. KNOWLES [1976] for a discussion of the isotropic case) and would require a careful derivation of anti–plane shear from the full three–dimensional theory, as in KNOWLES [1977].

For *isotropic* incompressible materials the shear stress response $\boldsymbol{\sigma}$ can be shown to depend only on $|\nabla u| = (u_x^2 + u_y^2)^{\frac{1}{2}}$ (cf. KNOWLES [1976]); in this case $W = W(|\nabla u|)$ and the stress–strain relationship simplifies to $\boldsymbol{\sigma}(\nabla u) = g(|\nabla u|^2)\nabla u$, with $g(\gamma^2) = W'(\gamma)/\gamma$. This implies that, in the absence of body forces or boundary effects, there is no preferred orientation of phase boundaries separating different phases. However, as the numerical examples in §6.2 and §6.3 indicate, for the dynamical problem under consideration, the boundary conditions, together with the initial conditions, can play an important rôle in selecting a few prominent phases.

Most studies of isotropic incompressible anti–plane shear have been concerned only with equilibrium solutions (see the references given above). A notable exception is the work

of ENGLER [1989] who showed the existence of mild as well as classical solutions to the dynamical anti–plane shear problem (2.13)–(2.15).

Following ROSAKIS [1992], we also introduce a class of idealized constitutive models for an anisotropic material possessing cubic symmetry, namely those having a shear stress response function of the form

$$\sigma(\nabla u) = (\sigma_1(u_x), \sigma_2(u_y)) \tag{2.16}$$

(here the coordinate axes provide the axes of cubic symmetry). Alternatively, we can define the stored energy functions $W_i(\gamma) = \int_0^\gamma \sigma_i(s)\,ds$ for $i = 1, 2$, so that $W(\nabla u) = W_1(u_x) + W_2(u_y)$ defines a stored energy density function with Fréchet derivative $DW(\nabla u) = \sigma(\nabla u)$.

We henceforth study the initial BVP (2.13)–(2.15), starting with a discussion and characterization of some equilibrium solutions, followed by existence and uniqueness results for the full problem in §3. We also attempt to generalize some of the results on the one–dimensional models due to BALL et al. [1991], and comment in §4 on the difficulties encountered.

2.3 Minimizing Sequences and Microstructures

For anti–plane shear the deformation gradient is completely described by the two–dimensional vector field $\nabla u : \Omega \to \mathrm{R}^2$, ensuring that any two homogeneous deformations can be rank–1 connected. Phenomena such as the wedge-like microstructures commonly observed in martensites (BALL & JAMES [1987], [1990], BHATTACHARYA [1991]), that are due to the incompatibility between phases not having a rank–1 connection (see (2.19) below), are therefore not expected to be observed in this model — in the absence of boundaries or strain discontinuities in the initial data there are no effects which promote the creation of such microstructure. However, unlike the one–dimensional models discussed in BALL et al. [1991], boundaries can produce non–trivial effects: there is no need for additional "displacement penalties" such as the final term in (2.6). We now consider the effect of zero displacement

boundary conditions on the creation of microstructure in the dynamic anti–plane shear problem.

As discussed in §2.1, we are primarily interested in stored energy functions $W(\nabla u)$ with multiple wells, which fail even to be rank–1 convex. Given a minimizing sequence $\{u_k\}$ of

$$I[u] = \int_\Omega W(\nabla u)\, \mathbf{dx} \tag{2.17}$$

in the admissible set

$$\mathcal{A} = \{u \in W^{1,p}(\Omega) : u = 0 \text{ on } \partial\Omega\}, \tag{2.18}$$

typical coercivity conditions on W, implying that $\|u_k\|_{W^{1,p}}$ is bounded, ensure the existence of a weakly convergent subsequence in the case $p < \infty$, and a weakly $*$ convergent subsequence in the case $p = \infty$ (cf. EVANS [1990]). The key questions are whether the limits of such subsequences are infima of $I[u]$ in the appropriate spaces, whether strongly convergent subsequences can be found, and, if the latter are ruled out, whether one can characterize the resulting microstructure (e.g. oscillations or singularities) and its effect on macroscopic physical quantities such as the energy, average strain, etc. The term "minimizer" has been used in various contexts and so, before stating our result, we define the notion of interest to us.

Definition 2.1 *A function $u \in \mathcal{A}$ which realizes the infimum of* (2.17)–(2.18) *will be called an absolute minimizer.*

We note that, where it is sufficiently smooth, such a minimizer must satisfy the Euler–Lagrange equation at all interior points of phase domains and the Hadamard jump condition on the remainder of Ω:

$$(\nabla \mathbf{u})^+ - (\nabla \mathbf{u})^- = \mathbf{a} \otimes \mathbf{n} \tag{2.19}$$

for some vector $\mathbf{a}$, where $\mathbf{n}$ is the normal to the interface. This rank–1 connection implies that interfaces between two distinct phases must be planar. For the scalar fields of anti–

plane shear (2.19) reduces to

$$(Vu)^{+} - (Vu)- = an \tag{2.20}$$

for a scalar a, and the interfaces are straight line segments.

Theorem 2.3 *Let W :Vu*-> W(Vu)* : $\mathbf{R}^2$ -> [0,oo) *be a local stored energy function with N distinct and nonzero potential wells at Vu* = Ai, ..., *AN, at which W(Aj)* = 0 *for all j.*

- *Case N* = 2: *For two distinct wells at A\ and* A2, *with A\ and* A2 *parallel and of opposite direction (implying that the origin lies in the open straight line segment connecting A\ and* A2j, *there exist piecewise affine minimizing sequences consisting of successively finer and finer alternating bands of the two phases. In this case, no absolute minimizer exists.*

- *Case N* $\geq$ 3: *// the triangle describing the open convex hull of any three distinct nonzero potential wells* Ai, A2 *and* A3 *has positive area and contains the origin, then minimizing sequences can be constructed which converge strongly to an absolute minimizer in* $W^{1,p}_{Q}(Q)$ *(p* < 00) *and weakly* in* $W^{1,\infty}_{Q}(Q)$, *and for which infinitesimally small structures are restricted to accumulate at the boundary. The smallest structures on any open set* fti C ft *can be chosen to have size* $\geq$ \ dist(fti,#ft).

Proof:

(Case *N* = 2) Assume Ai || A2 and of opposite direction. We first construct u_0 by sequentially alternating bands of thickness | Ai j"[1] consisting of the Ai phase with bands of thickness | A2 I"[1] consisting of the A2 phase. The Hadamard jump condition (2.19) implies parallel interfaces normal to both Ai and A2. Let n = Ai/ | Ai | and define

$$u_k(x) = u_0(k(x \cdot n)n + (x - (x \cdot n)n)) \tag{2.21}$$

for & = 1,2,... and x G ft. This is clearly a minimizing sequence for the energy /, i.e. /[tt*]~>0 and *Uk* satisfies the boundary condition in the (weak) limit (see Figure 3).

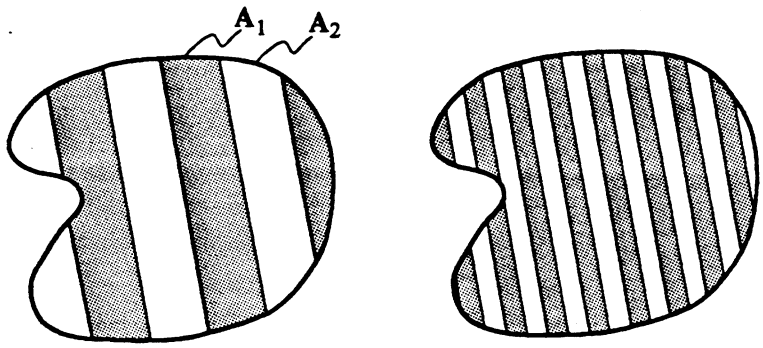

Figure 3: Two terms of a minimizing "twinning" sequence containing two phases.

Secondly, suppose that an absolute minimizer exists. Such a function u would necessarily realize the infimum $I[u] = 0$, implying that $\nabla u = \mathbf{A}_1$ or $\nabla u = \mathbf{A}_2$ a.e. Hence, from $u \in W_0^{1,p}(\Omega)$ (for some $p \geq 1$) it follows that $u \in W_0^{1,\infty}(\Omega) \subset C(\overline{\Omega})$. Since $\mathbf{A}_1$ and $\mathbf{A}_2$ are anti-parallel, there exists a unique linear, invertible change of coordinates $(x, y) = f(\xi, \eta)$, for which $\mathbf{A}_1 = f(1, 0)$ and $\mathbf{A}_2 = f(-\lambda, 0)$ for some $\lambda > 0$. In the new variables, $u \circ f \in C(\overline{f(\Omega)})$, and it therefore follows from $(u \circ f)_\eta = 0$ a.e. that $u \circ f$ is constant along lines parallel to the η-axis. Together with the boundary condition $u \circ f = 0$ on $\partial f(\Omega)$, this implies that $u \circ f = 0$ on $f(\Omega)$, and hence $u = 0$ on Ω. This contradicts the assumption that $\nabla u \neq 0$ a.e.

(Case $N \geq 3$) Let $\mathbf{A}_1$, $\mathbf{A}_2$ and $\mathbf{A}_3$ be three distinct nonzero phases satisfying the requirements of the claim and define the unit vectors $\mathbf{n}_{ij}$ normal to each (ij)–interface separating phases $\mathbf{A}_i$ and $\mathbf{A}_j$ (cf. Figure 4): i.e. $\mathbf{n}_{ij} = (\mathbf{A}'_i - \mathbf{A}'_j)/ \mid \mathbf{A}'_i - \mathbf{A}'_j \mid$, where $\mathbf{A}'_i = \mathbf{A}_i / \mid \mathbf{A}_i \mid^2$ is the reciprocal vector parallel to $\mathbf{A}_i$.

The two ways in which all three phases can meet in a point are shown in Figure 5(a). Choosing any of the constant u contours, we obtain a family of similar three-sided pyramids with identical orientations having negative (respectively positive) vertices whose (flat) bases correspond to triangles in Ω.

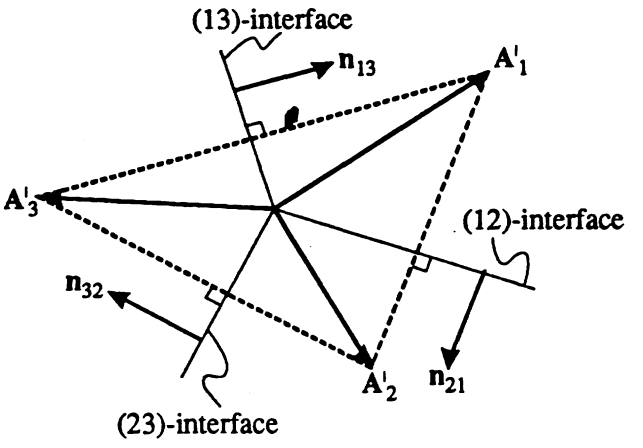

Figure 4: Orientation of the phase boundaries for three phases in strain space (u_x, u_y).

Choosing $u_0 \equiv 0$ as our starting point, we can build up a piecewise affine deformation by successively adding one of the two triangles, scaled to an appropriate size, in any region of Ω where $u \equiv 0$. Avoiding overlap, we can try to completely tile the domain and thereby obtain a piecewise affine u for which $\nabla u \in \{\mathbf{A}_1, \mathbf{A}_2, \mathbf{A}_3\}$ a.e. Except for special domains this will not be possible in a finite number of steps: we will require smaller and smaller tiles to fill in the gaps. We now show how to do this for a general domain, while limiting refinement to a layer adjacent to the boundary and having measure zero.

We first note that we can combine two triangles, one the reflection of the other, so as to obtain parallelograms of any size (cf. Figure 5(b)).

Choose P_0 to be such a parallelogram with diameter = 1 and let $\mathcal{M}_0$ be the two-dimensional lattice generated by the translates of P_0. We define $\mathcal{M}_k = 2^{-k}\mathcal{M}_0$, and will write P_k to denote any (closed) smallest parallelogram of $\mathcal{M}_k$ (i.e. $\mathrm{diam} P_k = 2^{-k}$). The domain Ω can be partitioned into the layers $\Omega_k = \{x \in \Omega : 2^{-k+1} < \mathrm{dist}(x, \partial\Omega) \leq 2^{-k+2}\}$ — since Ω is bounded we have $\Omega = \cup_{k=-K}^{\infty} \Omega_k$ for some finite $K > 0$.

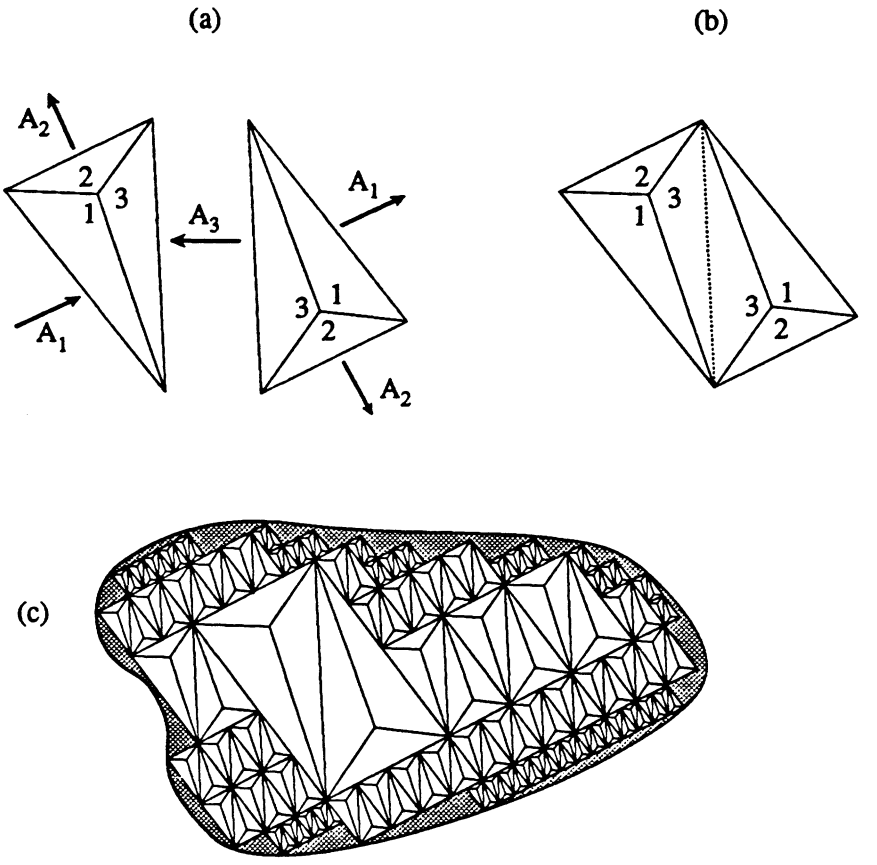

Figure 5: The proof of Theorem 2.3, $N \geq 3$. (a) Three phases meeting in a point; (b) Forming a parallelogram from two pyramids; (c) Construction of the minimizing sequence.

As our initial choice of tiles we take

$$\mathcal{P}_0 = \cup_k \{P_k \in \mathcal{M}_k : P_k \cap \Omega_k \neq \emptyset\}. \tag{2.22}$$

For any $P \in \mathcal{P}_0$, this ensures

$$\text{diam}P < \text{dist}(P, \partial\Omega) \leq 4\,\text{diam}P. \tag{2.23}$$

To see this, note that (2.22) implies the existence of some $x \in P \cup \Omega_k$ (for some k). Therefore $\text{dist}(P, \partial\Omega) \leq \text{dist}(x, \partial\Omega) \leq 2^{-k+2} = 4\text{diam}P$ and similarly we have $\text{dist}(P, \partial\Omega) > 2^{-k+1} - \text{diam}P = 2^{-k} = \text{diam}P$. This ensures that the parallelograms in $\mathcal{P}_0$ are all disjoint

from $\mathrm{R}^2\backslash\overline{\Omega}$ and that $\overline{\Omega} = \cup_{P\in\mathcal{P}_0}$.

However, the cover $\mathcal{P}_0$ does not exclude overlapping. To remove excessive tiles we observe that if any two parallelograms in $\mathcal{P}_0$ have overlapping interiors then one of the two must be contained in the other. From (2.22) and (2.23) it follows that each parallelogram has a unique maximal element in $\mathcal{P}_0$ which contains it, and that all maximal parallelograms will be disjoint. Taking $\mathcal{P}$ to be the collection of all maximal parallelograms in $\mathcal{P}_0$, we therefore obtain a partition of Ω that also satisfies (2.23).

For the nested sequence $\mathcal{P}_k = \mathcal{P}\cap(\cup_{l\le k}\mathcal{M}_l)$ we have $\limsup_{k\to\infty}\mathcal{P}_k = \overline{\Omega}$ and therefore $\lim_{k\to\infty}\mathrm{meas}(\mathcal{P}_k) = \mathrm{meas}(\overline{\Omega}) = \mathrm{meas}(\Omega)$, provided that the boundary has zero measure, which is the case for Lipschitz domains. (This construction is therefore also possible for certain domains with fractal boundaries.)

A minimizing sequence is constructed by taking u_k to be piecewise affine on $\mathcal{P}_k$ and $u_k \equiv 0$ on $\overline{\Omega}\backslash\mathcal{P}_k$. Let $u_\infty(x) = \lim_{k\to\infty} u_k(x)$ for $x\in\bar{\Omega}$. Since $\mathrm{meas}\{x\in\Omega : u_k(x) = 0\}\to 0$ as $k\to\infty$ it follows that $u_k \overset{*}{\rightharpoonup} u_\infty$ in $W_0^{1,\infty}(\Omega)$. Finally, since u_k is uniformly bounded in $W^{1,\infty}$ it also follows that $u_k\to u_\infty$ in $W_0^{1,p}(\Omega)$ for $p<\infty$. □

Remarks:

1. There are many other ways of constructing such tilings and the above minimizing sequences are clearly not necessarily the ones selected by the dynamics. They were nevertheless constructed so as to reflect the numerical observation that larger structures appear to "lock in" first with successively finer structures subsequently forming around the larger ones (see §6). That this is also a physically realizable scenario is suggested by the micrographs in VAN TENDELOO, VAN LANDUYT & AMELINCKX [1976] (especially Figure 8); see also Figure 6 in BALL & JAMES [1987]. Obviously more than three phases can be used in this process. An example is provided by the 4–well material which can construct ridges consisting of stacked pyramids, thereby achieving compatibility with the boundary, see Figure 20 below.

2. A different proof for the case $N = 2$ is given in CHIPOT [1991], where it is also shown that any minimizing sequence will define the Young measure (cf. TARTAR [1983]):

$$\nu_{\mathbf{x}} = \frac{|A_2|}{|A_1| + |A_2|}\delta_{A_1} + \frac{|A_1|}{|A_1| + |A_2|}\delta_{A_2} \quad \text{a.e. } \mathbf{x} \in \Omega,$$

where $Sj^{\wedge}_{:}$ denotes the Dirac mass at A_i.

3. The requirement, in the case of three or more wells, that the convex hull of the wells should have positive area and include the origin, is a constructive version of the following result on weak* convergence (cf. TARTAR [1983]): if Vu_k -^ Vt^ in $Z^{\circ\circ}(£2,R^2)$ and Vujt G K a.e., then VtXoo € closed convex hull of K. In order to satisfy the zero boundary conditions in this case it is therefore required that 0 be in the convex hull of the given finite number of wells.

4. Theorem 2.3 is clearly also valid if ft is a domain which can be expressed as a finite union of simply connected domains, each with a Lipschitz-smooth boundary. Thus the result also applies to some non simply connected domains.

5. For the isotropic problem with at least one nontrivial potential well (cf. §6.2 and §6.3) at $|Vw| = 7 > 0$, the last case of this theorem implies the existence of uncountably many minimizing sequences (compare also with the nonexistence results in BAUMANN & PHILLIPS [1990], who consider a much more restricted class of stored energy functions).

In §4 we discuss the question of whether the nonexistence of absolute minimizers can actually prevent solutions from minimizing the energy.

3 The Dynamical Problem

3.1 The Transformed Problem

RYBKA [1992] established global existence and uniqueness of solutions to the general n-dimensional problem

$$u_{tt} = \text{divr} = \text{div}(<\text{r}(Vu) + Vu_t), \tag{3.1}$$

which allows phase changes, and we will apply his approach to the dynamical anti–plane shear problem (2.13)–(2.15). Although the emphasis in RYBKA [1992] is on the traction–free boundary value problem, he indicates that his methods also apply to the Dirichlet boundary value problem. We now present the general L^p–extension of RYBKA's results and establish the existence, uniqueness and regularity of solutions for the Dirichlet problem.

The crucial step in RYBKA's work was his n–dimensional generalization of the one–dimensional transformation first used by ANDREWS [1980] and subsequently in ANDREWS & BALL [1982], in PEGO [1987] and (in a slightly modified form) in BALL et al. [1991]. Using this transformation (which depends on the boundary conditions), the equations of elastodynamics with viscoelastic damping (3.1) can be shown to be equivalent to a semi-linear degenerate parabolic system which can be analyzed by standard methods of semi-group theory and the theory of dissipative dynamical systems (as presented for example in HENRY [1981]). For the anti–plane shear problem (2.13)–(2.15), RYBKA's transformation involves finding the irrotational vector fields $\mathbf{P}, \mathbf{Q} : \Omega \to \mathrm{R}^2$ satisfying

$$div\mathbf{P} = u_t \quad \text{and} \quad \mathbf{P} + \mathbf{Q} = \mu \nabla u, \tag{3.2}$$

$$curl\mathbf{P} = curl\mathbf{Q} = 0. \tag{3.3}$$

The Dirichlet boundary condition $u_t = 0$ on $\partial\Omega$ becomes $div\mathbf{P} = 0$ on $\partial\Omega$, and (2.13)–(2.15) can be shown to be equivalent to the system

$$\begin{aligned} \mathbf{P}_t = \quad & \mu \nabla div\mathbf{P} \quad + \quad \pi_D \sigma((\mathbf{P}+\mathbf{Q})/\mu), \\ \mathbf{Q}_t = \quad & \qquad\qquad - \quad \pi_D \sigma((\mathbf{P}+\mathbf{Q})/\mu), \end{aligned} \tag{3.4}$$

with the projection $\pi_D = \nabla \Delta_D^{-1} div$, where $\Delta_D^{-1} f$ is the solution to the Poisson problem $\Delta v = f$ with $v = 0$ on $\partial\Omega$ (see Lemma 3.3 below). The initial conditions for the transformed problem are given by

$$\mathbf{P}(\mathbf{x}, 0) \equiv \mathbf{P}_0 \quad \text{with } div\mathbf{P}_0 = u_t|_{t=0}, \tag{3.5}$$

$$\mathbf{Q}(\mathbf{x},0) \equiv \mathbf{Q}_0 = \mu \nabla u|_{t=0} - \mathbf{P}_0. \tag{3.6}$$

Before we make this equivalence more precise, we first collect some results about the projection $\pi_D = \nabla \Delta_D^{-1} div$ for future reference.

Lemma 3.1 *Properties of the projection* $\pi_D = \nabla \Delta_D^{-1} div$.
π_D *is a projection on* $L^p(\Omega, \mathrm{R}^2)$ *for* $1 < p < \infty$, *i.e.* $\pi_D \in L(L^p(\Omega, \mathrm{R}^2))$ *and* $\pi_D^2 = \pi_D$, *with* $\pi_D L^p(\Omega, \mathrm{R}^2) = \{\nabla \phi : \phi \in W_0^{1,p}(\Omega, \mathrm{R})\}$ *a closed subspace of* L^p. *Hence, each* $\mathbf{P} \in \pi_D L^p$ *can be uniquely identified with the gradient of some potential* $\phi \in W_0^{1,p}$.

$(\pi_D \mathbf{f}, \mathbf{g}) = (\mathbf{f}, \pi_D \mathbf{g})$ *for* $\mathbf{f} \in L^p, \mathbf{g} \in L^{p'}, 1/p + 1/p' = 1$; *i.e.* $\pi_D |_{L^p}$ *is the adjoint of* $\pi_D |_{L^{p'}}$ *and* $(\pi_D L^p)' = \pi_D L^{p'}$.

$L^p = \pi_D L^p \oplus (\mathbf{I} - \pi_D) L^p$ *for* $1 < p < \infty$, *with orthogonality in the sense of the duality pairing between* L^p *and* $L^{p'}$. *For* $p = 2$, π_D *provides an* L^2*-orthogonal decomposition of* L^2.

Proof:

Although the above properties can be established directly, they also follow from the relationship between π_D and the Helmholtz projection for vector fields in L^p as developed in FUJIWARA & MORIMOTO [1977], see RYBKA [1992, Appendix]. Since the map $\nabla : W_0^{1,p} \to \pi_D L^p$ is an isomorphism, each $\mathbf{P} \in \pi_D L^p$ can be uniquely identified with the gradient of a potential ϕ in $W_0^{1,p}$. □

We next show that π_D acts as a Helmholtz-type projection by removing the rotational component from a vector field.

Lemma 3.2 *The map* $div : \pi_D L^p(\Omega, \mathrm{R}^2) \cap W^{1,p}(\Omega, \mathrm{R}^2) \to L^p(\Omega, \mathrm{R}^2)$ *is an isomorphism of Banach spaces, i.e. we have the following equivalence of norms:*

$$\|div \mathbf{P}\|_{L^p} \cong \|\mathbf{P}\|_{W^{1,p}} \quad \text{for } \mathbf{P} \in \pi_D L^p \cap W^{1,p}. \tag{3.7}$$

Proof:

From Lemma 3.1 we have the characterization

$$\pi_D L^p \cap W^{1,p} = \{\nabla\phi : \phi \in W_0^{1,p} \cap W^{2,p}\} = \pi_D W^{1,p}$$

and we therefore only need to show that $\|\Delta\phi\|_{L^p} \cong \|\nabla\phi\|_{W^{1,p}}$. Since $\phi \in W_0^{1,p}$ we obtain $\|\nabla\phi\|_{L^p} \cong \|\phi\|_{W^{1,p}}$ from Poincaré's inequality (ZIEMER [1989]), and since $\Delta : W_0^{1,p} \cap W^{2,p} \to L^p$ is an isomorphism of Banach spaces for all $p \in (1,\infty)$ (GRISVARD [1985]) (this requires only that Ω is bounded and that $\partial\Omega$ is $C^{1,1}$ or piecewise smooth without any re–entrant corners), we have $\|\Delta\phi\|_{L^p} \cong \|\phi\|_{W^{2,p}} \cong \|\nabla\phi\|_{W^{1,p}}$, proving the lemma. □

As in the one–dimensional case, transforming the problem into the $\mathbf{P}, \mathbf{Q}$ variables also makes the rôle of the viscoelastic dissipation more apparent. This dissipation is represented by the linear operator $\mu\nabla div$ in (3.4) and has a limited smoothing effect on the $\mathbf{P}$ component, while the absence of a similar term for the $\mathbf{Q}$ component in (3.4) indicates that initial discontinuities in $\mathbf{Q}$ — which via (3.2) correspond to initial discontinuities in the displacement gradient ∇u — need not be smoothed out by the dynamics (although we do not rule out the possibility that the nonlinearity can also cause some smoothing of singularities).

We now summarize the important properties of $A_p \equiv -\nabla div$, where $p \in (1,\infty)$ indicates that its domain $D(A_p)$ is chosen to lie in the base space $\pi_D L^p(\Omega, \mathrm{R}^2)$. The following Lemma extends the results in RYBKA [1992] to the case $p \neq 2$.

Lemma 3.3 *Properties of the operator ∇div*

The linear operator $A_p = -\nabla div$ with domain

$$D(A_p) = \pi_D L^p \cap \{\mathbf{P} \in W^{2,p}(\Omega, \mathrm{R}^2) : div\mathbf{P} = 0 \text{ on } \partial\Omega\}$$

provides an isomorphism from $D(A^p)$ to $\pi_D L^p$.

A_p is a sectorial operator with $D(A_p^{\frac{1}{2}}) = \pi_D W^{1,p}$. If $p = 2$, A_2 is selfadjoint and positive definite.

Proof:

A_p is the composition of the two isomorphisms, $div : D(A_p) \to W_0^{1,p}$ and $\nabla : W_0^{1,p} \to \pi_D L^p$, and is therefore an isomorphism from $D(A_p)$ to $\pi_D L^p$. The proof that A_p is sectorial follows exactly as in the proof (RYBKA [1992, Theorem 3.1]) that the associated linear operator with Neumann boundary condition is sectorial. The only difference is that here we appeal to Lemma 3.2 instead of RYBKA [1992, Lemma 2.3].

We now show that $D(A_p^{\frac{1}{2}}) = \pi_D W^{1,p}$. For $p = 2$ the selfadjointness of A_2 (Lemma 3.3) gives the associated bilinear form $(A_2\mathbf{P}, \mathbf{P}) = \|div\mathbf{P}\|^2$. By Lemma 3.2 this provides an inner product on the space $\pi_D W^{1,2}$ and it therefore follows (KATO [1966, Theorem VI.2.23]) that $A_2^{\frac{1}{2}}$ is selfadjoint with domain $D(A_2^{\frac{1}{2}}) = \pi_D W^{1,2}$. For general $p \in (2, \infty)$ we have from TRIEBEL [1978, Theorem 1.15.3/1] that $D(A_p^{\frac{1}{2}}) = [\pi_D L^p, D(A_p)]_{\frac{1}{2}}$; where the square brackets indicate complex interpolation. The above characterization of $D(A_p)$, together with TRIEBEL [1978, Theorem 1.17.1/1], gives

$$\begin{aligned} [\pi_D L^p, D(A_p)]_{\frac{1}{2}} &= \left[\pi_D L^p \cap L^p, \pi_D L^p \cap \{\mathbf{P} \in W^{2,p} : div\mathbf{P} = 0\}\right]_{\frac{1}{2}} \\ &= \pi_D L^p \cap \left[L^p, \{\mathbf{P} \in W^{2,p} : div\mathbf{P} = 0\}\right]_{\frac{1}{2}}. \end{aligned}$$

The boundary condition does not survive the process of interpolation (TRIEBEL [1978, Theorem 4.3.3/1]), and it therefore follows from TRIEBEL [1978, Theorem 4.3.2/2] that

$$D(A_p^{\frac{1}{2}}) = \pi_D L^p \cap [L^p, W^{2,p}]_{\frac{1}{2}} = \pi_D L^p \cap W^{1,p} = \pi_D W^{1,p}.$$

That A_2 is self-adjoint and positive definite (and therefore also sectorial) is shown in RYBKA [1992, Theorem 3.7 and Proposition 3.8]. □

We now show that a solution to the transformed system (3.4) delivers a unique solution to the original problem (2.13)–(2.15).

Lemma 3.4 *If* $(\mathbf{P}, \mathbf{Q})$ *is a weak solution of the transformed system* (3.4) *that satisfies, for*

some p,q G (l,oo),

$$P \in C([0,T), *_D L^{*} \cap W^{1}*), \quad Q \in C([0,T), *_D L»), \tag{3.8}$$

$$P_t \in C([0,T), \nabla r_D L^{*} \cap W^{1,''}), \quad Q_t \in C((O,T), XDL«), \tag{3.9}$$

$$\nabla \cdot D(A_q) \text{ forte } (0,T), \tag{3.10}$$

tfeen t/iere *exists a unique weak solution u to the original anti-plane shear problem* (2.13)-(2.15), *which satisfies*

$$u_u Vue \in C([0,T), L^p), \quad u_t = 0 \text{ on } 0ft, \tag{3.11}$$

$$/iVtt_t + \nabla TDa(Vu) \in C((0,T), TT_D I^9 \cap W^{1} \wedge), \tag{3.12}$$

and is related to the transformed system (3.4) *via* (3.2).

Proof:

We can set /x = 1 without any loss of generality. With $u_t = divP$ and F = P + Q, Lemma 3.2 implies that

$$P \in C([0,r), iri)2; *\cap W^{1}*) \text{ and } Q \in C([0,T), irz > I^p)$$

if and only if

$$u_t \in C([0,T), X^p) \text{ and } F \in C([0,T), TT_D I^p).$$

To see that F = Vu, we note that (3.4) implies $F_t = P_t + Q_t = VdivP = Vw_t$; this also gives $Vu_t \in C((0,r), 7T£) I^9)$. The boundary condition $u_t = 0$ follows from P G i?(A_g) for t > 0 and the characterization of $D(A_q)$ in Lemma 3.3. Finally, from the P equation in (3.4) we have $ir_D(r \in C((0,T), TT_D Z, P \text{ fl } VF^{1,9})$ and therefore

$$utt = div(VdivP + ir \wedge cr) = dtv(Vnt + cr) \in C((0,T), X^9),$$

which shows that u is a solution to the original problem. D

The projection TID is closely related to the Helmholtz decomposition of a vectorfield into its divergence-free and curl-free (irrotational) components. For example, let TT// be

the Helmholtz projection which maps a vectorfield $\mathbf{f} : \Omega \to \mathrm{R}^2$ uniquely to a divergence free vector field that vanishes on the boundary, i.e. $\pi_H \mathbf{f} = \mathbf{0}$ on $\partial\Omega$. In the framework of fluid dynamics, $\pi_H \mathbf{f}$ often represents the velocity field of an incompressible fluid contained in the domain Ω, with no penetration or slip on the boundary. Then $\pi_H = \mathbf{I} - \pi_D - \pi_0$, with π_D as above and $\pi_0 \mathbf{f} = \nabla\phi$, where ϕ is the harmonic solution to the Poisson problem $\Delta\phi = 0$ in Ω, $\partial\phi/\partial n = (\mathbf{I} - \pi_D)\mathbf{f} \cdot \mathbf{n}$ on $\partial\Omega$.

The relevance of the Helmholtz decomposition $\mathbf{I} = \pi_H + \pi_D + \pi_0$ for the equations of elastodynamics $u_{tt} = div\tau$, where τ represents the total stress, follows from the observation that the dynamical evolution of the material is fully determined by the divergence of τ, and is unaffected by the addition of an arbitrary irrotational vector field (or, more generally, a tensor field) to τ.

We do not know whether this projection is merely a technical device or has a "natural" physical significance. However, we remark that general constitutive laws, e.g.

$$\tau : (\nabla u, \nabla u_t) \mapsto \sigma(\nabla u) + \mu \nabla u_t, \tag{3.13}$$

with nonlinear σ can destroy the gradient form of the vector fields ∇u and ∇u_t. The projection $\pi_D \tau = \pi_D \sigma$ effectively selects the part of the total stress which, via the divergence, drives the dynamics. This is a nonlocal operation.

Alternatively, one can view (3.4) as a dynamical attempt at minimizing the potential energy $I = \int_\Omega W(\mathbf{F})\, \mathbf{dx}$ under the constraint that $\mathbf{F}$ must correspond to the gradient of some scalar function u with $u = 0$ on $\partial\Omega$. Since $\sigma(\mathbf{F}) = \partial W(\mathbf{F})/\partial(\mathbf{F})$, $-\sigma(\mathbf{F})$ represents the "direction of steepest descent" for the unconstrained problem. However, adding the constraint severely limits the allowable directions along which $\mathbf{F}$ can relax in an effort to decrease the total stored elastic energy I. Writing $\nabla u = \mathbf{F}$, the $\mathbf{Q}$-component of (3.4) can be written as

$$\mu \mathbf{F}_t = -\pi_D \sigma(\mathbf{F}) + \mathbf{P}_t, \tag{3.14}$$

and in the presence of a large viscoelastic damping $\mu >> 1$, and a corresponding rapid decay of the energy I, we can change to the "fast" time $\tau = t/\mu$, giving

$$\mathbf{F}_\tau = -\boldsymbol{\pi}_D\boldsymbol{\sigma}(\mathbf{F}) + \frac{1}{\mu}\mathbf{P}_\tau \approx -\boldsymbol{\pi}_D\boldsymbol{\sigma}(\mathbf{F}) \tag{3.15}$$

($\mathbf{P}_t$ can be shown to decay to zero as $t\to\infty$). This justifies interpreting $-\boldsymbol{\pi}_D\boldsymbol{\sigma}(\mathbf{F})$ as the direction of steepest descent along the constraint curves.

The appropriate choice of such a change of variables, which transforms the problem of interest into a more accessible semilinear parabolic system of PDEs, underlies much of the analysis of ANDREWS [1980], ANDREWS & BALL [1980], PEGO [1987], BALL et al. [1991] and RYBKA [1992]. This raises the question of whether similar transformations can be derived in a more systematic fashion and for a larger class of problems. We now generalize and consider the class of problems given by

$$u_{tt} = Au_t + div\mathbf{T} \tag{3.16}$$

where A is a general invertible linear operator, $\mathbf{T}$ contains the nonlinear terms and u can be scalar, vector or tensor. We will show that the transformations employed, in (3.2)–(3.4) and the above references, can all be viewed as derived from a formal diagonalization of the linear part of (3.16).

By setting $v = u_t$ we obtain the semilinear "first order" system

$$\begin{bmatrix} u_t \\ v_t \end{bmatrix} = \begin{bmatrix} 0 & I \\ 0 & A \end{bmatrix}\begin{bmatrix} u \\ v \end{bmatrix} + \begin{bmatrix} 0 \\ div\mathbf{T} \end{bmatrix}, \tag{3.17}$$

whose linear part can be diagonalized by means of a linear change of variables. Elementary matrix algebra gives this diagonalization as

$$B^{-1}\begin{bmatrix} 0 & I \\ A & -I \end{bmatrix}\begin{bmatrix} 0 & I \\ 0 & A \end{bmatrix}\begin{bmatrix} A^{-1} & A^{-1} \\ I & 0 \end{bmatrix}B = \begin{bmatrix} B^{-1}AB & 0 \\ 0 & 0 \end{bmatrix}, \tag{3.18}$$

with B an arbitrary invertible linear operator which need not commute with A. The associated transformation to the new variables p and q is given by

$$\begin{bmatrix} p \\ q \end{bmatrix} = B^{-1} \begin{bmatrix} 0 & I \\ A & -I \end{bmatrix} \begin{bmatrix} u \\ v \end{bmatrix}, \tag{3.19}$$

or, equivalently, $u_t = v = Bp$ and $p + q = B^{-1}Au$. This transforms the original problem (3.16) into the form

$$\begin{bmatrix} p_t \\ q_t \end{bmatrix} = \begin{bmatrix} B^{-1}AB & 0 \\ 0 & 0 \end{bmatrix} \begin{bmatrix} p \\ q \end{bmatrix} + B^{-1} div \mathbf{T} \begin{bmatrix} I \\ -I \end{bmatrix}, \tag{3.20}$$

which shows that a further simplification in the nonlinear term is possible by choosing $B = div$. It is in this choice that the boundary conditions will play a crucial rôle. We therefore see that the "algebraic" relations $u_t = div\, p$ and $p + q = \nabla u$ — which are encountered, in one form of another, in all of the above works — result directly from the diagonalization, whilst the particular choice of spaces and projection operators onto these spaces are necessary for the transformed problem to be well–posed as a semilinear parabolic PDE.

Remark: Regularization methods involving capillarity or second order strain gradients result in the addition of a term $\triangle\triangle u$ to the evolution equations (2.11) and (2.13). Transforming as above, this leads to the same nonlinearity, but with a strictly dissipative linear operator in (3.20).

3.2 Existence, Uniqueness and Regularity of Solutions

The global existence of unique strong solutions to the anti–plane shear problem in its transformed form and with a globally Lipschitz continuous stress–strain response follows as in RYBKA [1992, Theorem 3.7] (although he only sketches the proof for the case $p = 2$). We present a slightly sharper version which is valid for all $p \in [2, \infty)$.

Theorem 3.1 *Global existence and uniqueness.*

For a globally Lipschitz continuous stress–strain response σ *and initial data* $\mathbf{P}_0 \in \pi_D W^{1,p}$ *and* $\mathbf{Q}_0 \in \pi_D L^p$*, there exists a unique global solution to the transformed boundary value problem* (3.2)–(3.7) *with*

$$\mathbf{P} \in C\left([0,\infty), \pi_D W^{1,p}\right) \cap C^1\left((0,\infty), C^\nu\right) \cap C\left((0,\infty), D(A_p)\right), \quad \text{for all } 0 \le \nu < 2(1-1/p), \tag{3.21}$$

$$\mathbf{Q} \in C\left([0,\infty), \pi_D L^p\right) \cap C^1\left((0,\infty), \pi_D L^p\right). \tag{3.22}$$

Proof:

We write $z = \{\mathbf{P}, \mathbf{Q}\}$, $Bz = \{\mu A_p \mathbf{P}, \mathbf{0}\}$ and $f(z) = \pi_D \sigma((\mathbf{P}+\mathbf{Q})/\mu)\ \{1, -1\}$ and treat (3.2)–(3.6) as the abstract parabolic equation

$$z_t + Bz = f(z) \tag{3.23}$$

on the Banach space $X = \pi_D L^p \times \pi_D L^p$. That B is a sectorial operator follows from the diagonal structure of B and the sectoriality of A_p (Lemma 3.3). As in the one–dimensional problem we therefore have that $D(B^\alpha) = D(A_p^\alpha) \times \pi_D L^p$ (i.e. the resulting linear semigroup causes no smoothing in the $\mathbf{Q}$–component). We choose $\alpha = \frac{1}{2}$ and use the fact from Lemma 3.3 that $D(A_p^{\frac{1}{2}}) = \pi_D W^{1,p}$.

As in the case with Neumann boundary conditions (RYBKA [1992, Theorem 3.1]), it follows from the assumption that σ is globally Lipschitz continuous and the fact that π_D is a projection operator on L^p (Lemma 3.1), that

$$f : D(B^{\frac{1}{2}}) = \pi_D W^{1,p} \times \pi_D L^p \to \pi_D L^p \times \pi_D L^p \tag{3.24}$$

is a globally Lipschitz continuous map. Theorems 3.3.3 and 3.5.2 of HENRY [1981] (together with the modification in MIKLAVČIČ [1985]) therefore yields a local solution

$$z \in C([0,T), X^{\frac{1}{2}}) \cap C^1((0,T), X^\gamma) \cap C((0,T), D(B)) \tag{3.25}$$

for all $7 < 1$ and some $T > 0$. Here $X'' * = D(B''^{|f})$ (see HENRY [1981]) and from HENRY [1981, Theorem 1.6.1] we have that $D\{A\})$ C C for $0 \leq v < 2(7 - i)$. In terms of $\{P, Q\}$, this implies that, for all $0 \leq v < 2(1 - \frac{1}{p})$,

$$FeC\ ([0, T), n_D W^{\wedge})\ \text{n}\ C^1\ ((0, T), T\ D\ C\ )\ \text{n}\ C\ ((0, T), Z?(A_P)), \tag{3.26}$$

$$Q\ e\ c\ ([0, T), *_D V)\ \text{n}\ c^1\ ((o, r), \text{ir}_o\text{i}''). \tag{3.27}$$

The assumption that / is globally Lipschitz continuous allows us to estimate

$$||/(x)||_x\ \text{SifCl} + \text{IMI}^{\wedge}) \tag{3.28}$$

and therefore appeal to HENRY [1981, Corollary 3.3.5] to establish global existence of solutions. Uniqueness follows in a standard fashion by subtracting two solutions and using the global Lipschitz continuity of a together with Gronwall's inequality. D

Note that, by Lemmas 3.2 and 3.4, we have therefore shown the existence of global solutions to the original anti-plane shear problem (2.13)-(2.15) with

$$u_t\ \ e\ \ \text{C}([\text{o},\text{oo}),^{\wedge})\text{nc}^1((\text{o},\text{oc}),\text{y})\text{nc}((\text{o},\text{oo}),\text{iy}_0{}^{1,\text{p}}), \tag{3.29}$$

$$Vu\ \ €\ \ C([0,oo)_J ir_D L^p) DC^1((0_i oo), ic_D L^p), \tag{3.30}$$

where $Y = L^q$ for any $q < oo$ if $p = 2$, and $Y = C^c$ for any $€ < 1 - 2/p$ if $p > 2$.

We observe that this proof requires very little of the nonlinear term /, and hence of the constitutive law o, other than it be globally Lipschitz. However, as we discuss in §4.1, this restriction excludes many realistic material models. Nor does the proof give any information regarding boundedness of solutions. A priori bounds may be obtained by considering the evolution of total energy:

$$E = \|\|u_t\|\|^2 + / W(Vu)\ \text{dx} \tag{3.31}$$

$$= \tfrac{1}{2}\|div\mathbf{P}\|^2 + \int_\Omega W((\mathbf{P} + \mathbf{Q})/\mu)\ \text{dx}. \tag{3.32}$$

As in the one–dimensional example, a direct calculation shows that

$$\frac{dE}{dt} = -\mu \|\nabla u_t\|^2 \tag{3.33}$$

on solutions, and hence that E is nonincreasing. If $W(\nabla u)$ satisfies a reasonable growth condition such as (4.1) below, then the bounds on E and (3.33) imply that $\|u_t\| = \|divP\|$ and $\|\nabla u\|_{L^p} = \|(\mathbf{P} + \mathbf{Q})/\mu\|_{L^p}$ (for some $p < \infty$) are bounded above for all time. This does not, of course, rule out the possibility of stress concentrations in which $\|\nabla u\|_{L^q}$ for some $q > p$ or even $\|\nabla u\|_\infty$ become unbounded (perhaps in finite time), but it gives some global stability information. Also see §4.1 below.

Linear stability results of the type discussed in BALL et al. [1991] for one–dimensional problems may also be obtained. For the problem with traction–free boundary conditions RYBKA [1992, Theorem 5.7] proves a restricted version of stability for certain smooth stored local elastic potentials W possessing two isolated but rank–1 connected local minima. As in the results for the one- dimensional models, this holds only for continuous perturbations, under which discontinuities do not move. However, it is unclear if such results are relevant in the case of anti–plane shear, since it is unlikely that this restricted class of motions is itself stable within the larger space of three-dimensional perturbations.

4 Some Open Problems

4.1 On Growth Conditions and Alternative Strategies

RYBKA's results and their generalization in Theorem 3.1 above, are the first for general constitutive laws σ, permitting phase changes of the type of interest in this work. However, the above existence proof and the results of RYBKA on which it is based, is restricted in that it only applies to constitutive laws for which σ is globally Lipschitz. In the case of anti–plane shear it can be argued that this constitutive constraint, and the upper bound on wave speeds that it implies, is no less realistic than the assumption of incompressibility.

Nevertheless, more general coercivity and growth conditions of the form

$$c + d|\mathbf{F}|^p \leq W(\mathbf{F}) \leq C + D|\mathbf{F}|^p\,, \quad \text{with } d, C, D > 0 \tag{4.1}$$

have played an essential rôle in the analysis of specific boundary value problems of nonlinear elasticity (cf. ANTMAN [1983] and the references therein), and it is therefore natural to try and extend the above results and those of RYBKA to this case. However, even in the special case of anti–plane shear one encounters serious problems in such an attempt.

The assumption that $\boldsymbol{\sigma}$ is globally Lipschitz continuous is essential in the proof of Theorem 3.1, as in RYBKA [1992], for both local and global existence. Local existence relies here on a contraction mapping principle which requires $\boldsymbol{\sigma}$ to be at least locally Lipschitz continuous (HENRY [1981, Theorem 3.3.3]), whilst global existence follows from Gronwall's inequality (HENRY [1981, Theorem 3.3.5]), which in this case merely ensures that the solution do not blow up in finite time. For a more general stress–strain relationship $\boldsymbol{\sigma}$ corresponding to (4.1) this method therefore fails at the outset.

In an attempt to overcome problems associated with the polynomial–type growth of the more general W in (4.1), one can try using a Faedo–Galerkin approach. However, this line of attack fails in a different manner: the nonconvexity of W (due to multiple potential wells) prevents passing the weak limit of the resulting Faedo–Galerkin approximating sequence (in successively higher but always finite dimensional spaces) through the nonlinearity. This problem is made more severe by the fact that we only have an ODE in $\mathbf{Q}$, which results in rather weak a priori estimates for the Faedo–Galerkin approximation of the $\mathbf{Q}$ component.

An alternative approach would be to show that, for certain constitutive laws, the solution avoids the formation of stress concentrations, and that the displacement gradient never explores the regions of the constitutive laws corresponding to arbitrarily large strains. This was possible in one dimension, and L^∞ estimates were obtained by using geometric contraction arguments on the q–equation (see PEGO [1987] and BALL et al. [1991]). The

aggressively nonlocal nature of the projection $\pi_D = \nabla \Delta_D^{-1} div$ in n–dimensions makes the exploitation of geometric information very problematic, even for simple choices of σ, as in the cases chosen for numerical work. However, the local properties of projections such as π_D have received very little attention and progress may be possible here, at least for suitably chosen boundary conditions, constitutive laws and geometries.

4.2 Strain Discontinuities and Energy Minimization

In the one–dimensional case, the transformation to the variables p, q made it possible to show that strain discontinuities (i.e. jumps in u_x) cannot be created or destroyed in finite time, and therefore cannot migrate into regions of continuity in u_x (Theorem 2.2 above). It is interesting to note that this property also holds in higher dimensions, at least for the strongly damped linear wave equation

$$u_{tt} + \alpha A u_t + A u = 0 \quad \text{on } \Omega, \tag{4.2}$$

$$u = 0 \quad \text{on } \partial\Omega, \tag{4.3}$$

where A is a self–adjoint, positive definite, linear elliptic partial differential operator (PDO) of second order with smooth coefficients, and α is a fixed constant (LARSSON, THOMEÉ & WAHLBIN [1991]). Under slightly more restrictive assumptions, this result can even be extended to the general linear problem

$$u_{tt} + A u_t + B u = 0 \quad \text{on } \Omega, \tag{4.4}$$

$$u = 0 \quad \text{on } \partial\Omega, \tag{4.5}$$

where B is an at most second order linear PDO with sufficiently smooth coefficients and provided that one restricts attention to an interior subdomain of Ω which does not touch the boundary $\partial\Omega$ (WAHLBIN [1991]). This, together with the numerical evidence presented in §6, is strongly suggestive that the viscoelastic damping prevents the propagation of strain

discontinuities in the (nonlinear) anti-plane shear problem. However, when attempting to generalize the one-dimensional result to the (two-dimensional) anti-plane shear problem, one is faced with the fundamental problem of choosing an appropriate function space in which to study the propagation of discontinuities (for the above linear problems this is avoided due to the existence of an explicit representation of the solution). Although $L^{\circ\circ}$ suffices for the one-dimensional case, it fails here since $irpL \wedge fcL^{00}$ (this follows from the fact that $A5^1I^{OO}£VF^{2,00}$ in two and higher dimensions). The Sobolev spaces $VF^{1\wedge}$, with p > 2, do not allow jump discontinuities in Q and hence in Vtt (by standard imbedding theorems) and are therefore also inappropriate. Possible alternative choices are the spaces of functions having bounded variation (BV) (cf. ZIEMER [1989]), bounded mean oscillation (BMO) and the appropriate Besov spaces (cf. BENNET & SHARPLEY [1988]), but in these cases either the physical interpretation is unclear or the semigroup theory underdeveloped, or both. We also remark that this problem of choosing a function space which generalizes the class of piecewise smooth functions, is a basic problem in hyperbolic systems of conservation laws (cf. DAFERMOS [1983]).

In addition, we remark that the proof of the persistence of strain discontinuities in the one-dimensional models of BALL et al. [1991] relies to a large extent on the fact that the projection merely removes a smooth component (here the average) and therefore cannot directly influence the evolution of strain discontinuities. In higher dimensions this is no longer true, as the projection 1 — TIE> acts nonlocally and without any apparent smoothing.

It was shown in BALL et al. [1991] (Theorem 2.1 above) that the related one-dimensional model (2.6) cannot possess any solutions which minimize the energy. The proof of this result involved showing that in this case minimization implies pointwise stabilization, and therefore the existence of an absolute minimizer, contradicting the fact that no such minimizer exists for this problem. This motivates the following question: can a solution to the anti-plane shear problem (or the general n-dimensional problem) minimize energy if the associated

total stored energy functional does not possess an absolute minimizer? Proceeding as in the proof for the one–dimensional case, we first note that minimization implies that $\mathbf{P}+\mathbf{Q}$ must converge in measure to the potential wells of W as $t\to\infty$. For smooth stored energy functions W which satisfy the growth condition

$$d + c|\mathbf{F}|^2 \leq W(\mathbf{F}) \leq D + C|\mathbf{F}|^2, \;\; c, C, D > 0 \tag{4.6}$$

it follows as in RYBKA [1992, Theorem 4.6] that $\mathbf{P}\to\mathbf{0}$ in $W^{2,2}$ as $t\to 0$, and we can therefore deduce that $\mathbf{Q}$ converges in measure to the potential wells (we note that (4.6) is the natural growth condition if σ is globally Lipschitz continuous). For smooth W possessing locally convex potential wells we therefore have that $\mathbf{Q}$ converges in measure to the potential wells of W and therefore also to the (isolated) zeroes of σ. However, contrary to the one–dimensional case, this is not sufficient to show that $(\mathbf{1}-\pi_D)\sigma\to\mathbf{0}$ in any space which will allow us to conclude (as in the one–dimensional case) that the $\mathbf{Q}$ component of (3.4) satisfies the asymptotically autonomous ODE $\mathbf{Q}_t = -\sigma(\mathbf{Q})$ as $t\to\infty$, which in turn would imply pointwise convergence of $\mathbf{Q}$ and thereby give the required contradiction. Clearly, the lack of knowledge about the pointwise action of the projection π_D makes the question of energy minimization much more subtle than in the one–dimensional case.

In §6 we present numerical simulations of dynamical problems both with and without absolute minimizers, as characterised in Definition 2.1 and Theorem 2.3. The evidence is suggestive of failure to minimize in the latter case (two–well potential) and of minimization in the former (potentials with three or more wells surrounding the origin, and isotropic potentials). We discuss this further in §7.

5 A Numerical Algorithm

In this section we describe a finite difference approach to the numerical solution of the above dynamical anti–plane shear problem. We utilize a finite difference spatial discretiza-

tion together with an adaptive timestepping scheme. Here the viscoelastic damping is incorporated in an implicit fashion and the nonlinear stress response in an explicit fashion. At each time step the resulting linear system is iteratively solved using a preconditioned conjugate gradient method.

We were unable to find any theoretical results that establish the accuracy or even the convergence of numerical solutions to the general problem (2.13)–(2.15), derived from a non–convex stored energy function. The isotropic problem is considered in FRENCH & WAHLBIN [1991], who establish optimal order error estimates for spatial finite element discretization (sub–optimal in the case of piecewise linear finite elements). In their study time discretization is handled by an "energy–preserving" scheme.

In establishing the specific form of the methods presented here, we were guided by classical approaches to the linearized problem (CANUTO, HUSSAINI, QUARTERONI & ZANG [1988], MEIS & MARCOWITZ [1981]), the practical experience gained with related nonlinear problems in the engineering literature (SACHDEV [1987], WOOD [1990]) and by numerically experimenting with various schemes for the linearized as well as the fully nonlinear equations. We first describe discretization in time and then, seperately, discretization in space.

Let $\delta t > 0$ be the time step and define

$$u^\nu(x,y) = u(x,y,\nu\delta t),\ \nu = 0,1,\ldots \tag{5.1}$$

to be the value of the solution at each time step. Solutions to (2.13)–(2.15) are smooth in time (see Theorem 3.1) and it therefore makes sense to use a finite difference approximation for the velocity u_t which is first order in time. The acceleration u_{tt} is approximated by the central difference scheme

$$u_{tt} \approx (u^{\nu+1} - 2u^\nu + u^{\nu-1})/\delta t^2, \tag{5.2}$$

and the viscoelastic damping is approximated by the implicit Euler method (cf. WOOD [1990])

$$\mu\triangle u_t \approx \mu(\triangle u^{\nu+1} - \triangle u^\nu)/\delta t. \tag{5.3}$$

This choice was motivated by the following observation. Numerical experiments with the anti–plane shear problem as well as with other one–dimensional models of BALL et al. [1991] reveal an initial stage of rapid pattern selection during which the larger structures set in and the finer structures, present in the initial data, seem to disappear (provided they are smooth). The latter information is not lost, however, as it plays an important rôle in the long term evolution and creation of microstructure. A simple and striking example of this numerical manifestation of sensitive dependence on initial conditions was presented in HOLMES & SWART [1991]. It implies that care should be taken to accurately capture the dynamical evolution of the high modes. In this respect, the implicit Euler method seems to be an appropriate choice.

The nonlinear stress response $div\sigma(\nabla u)$ is incorporated in an explicit fashion. This results in the one–stage two–step implicit algorithm

$$(u^{\nu+1} - 2u^{\nu} + u^{\nu-1})/\delta t^2 = div\sigma(\nabla u^{\nu}) + \mu(\triangle u^{\nu+1} - \triangle u^{\nu})/\delta t \tag{5.4}$$

or

$$(I - \mu\delta t\triangle)u^{\nu+1} = (2I - \mu\delta t\triangle)u^{\nu} - u^{\nu-1} + \delta t^2 div\sigma(\nabla u^{\nu}), \tag{5.5}$$

requiring at each time step the full solution at the previous two time steps. Although u^0 is easily obtainable from the given initial data $u(x, y, 0)$, an additional approximation to the initial velocity $u_t(x, y, 0)$ is required, so as to be able to start the algorithm. In an effort to preserve the first order (in time) accuracy of the approximation to u_t, we introduce the fictitious term u^{-1}, representing the solution at $t = -\delta t$, and employ the centered–difference approximation

$$u_{t|_{t=0}} \approx (u^1 - u^{-1})/2\delta t \tag{5.6}$$

to give

$$u^1 = u^{-1} + 2\delta t u_{t|_{t=0}}. \tag{5.7}$$

Together with (5.5) at $v = 0$ this provides an expression for ti[1], namely

$$(2/ - fiSt\ A)u^{l} = (21 - pit\ A)u\ \backslash_{ts0} + 26t\ u_t\ |_{t=o} + \delta t^2 div\sigma(\nabla u\ |_{t=0}), \tag{5.8}$$

which we use to start marching in time.

By assumption each u^v satisfies the boundary conditions, so that at each time step $t = u6t$ we can obtain it''^{*1} by solving a well-posed elliptic boundary value problem containing u^v and $u^{1''''1}$ as data. This motivates the following spatial discretization.

For some mesh size ft > 0 we define the regular two-dimensional grid on the lattice $\{(x, y) = (ift,jft),0 \leq i, j \leq j^\wedge\}$ (we restrict ourselves to the square domain for the sake of simplicity). We use $u\tilde{j}j$ to denote the finite difference approximation of the solution u at $x = ift, y = jh$ and $t = vbi$. The Dirichlet boundary conditions are imposed by choosing $N = I/ft$ to be an integer and requiring that, for all $v = 0, 1, \ldots,$

$$u\backslash_{\tilde{j}} = 0 \quad \text{for} \quad z\backslash j = 0 \text{or TV}. \tag{5.9}$$

The action of the Laplacian $t\backslash u^v$ is approximated by the usual 5-point difference molecule:

$$Att''(\tilde{t}fc,ifc)«^i?^<_{>j}, \tag{5.10}$$

where $D\backslash$ denotes the finite difference operator

$$D_h^2 u_{i,j}^v \equiv u_{i+1,j}^v + <_{\_w} + <_{J+1} + <,-\_! - 4H\&: \tag{5.11}$$

As we mentioned in §2.2, in addition to isotropic constitutive laws we will also investigate stress-strain response functions a which are of the form

$$\wedge(Vit) = (cri(ti_x), a_2(tt_y)), \tag{5.12}$$

although more general constitutive laws can also easily be handled with the current approach. For the divergence term $diva(Vu) = C\backslash(u_x)_x + O2(u_y)_y$ we therefore use the

conservation–form finite difference approximations

$$\sigma_1(u_x^\nu)_x \,|_{\substack{x=ih \\ y=jh}} \approx \sigma_{1_{i,j}}^\nu \equiv \frac{1}{h}\left[\sigma_1\left(\frac{u_{i+1,j}^\nu - u_{i,j}^\nu}{h}\right) - \sigma_1\left(\frac{u_{i,j}^\nu - u_{i-1,j}^\nu}{h}\right)\right], \tag{5.13}$$

$$\sigma_2(u_y^\nu)_y \,|_{\substack{x=ih \\ y=jh}} \approx \sigma_{2_{i,j}}^\nu \equiv \frac{1}{h}\left[\sigma_2\left(\frac{u_{i,j+1}^\nu - u_{i,j}^\nu}{h}\right) - \sigma_2\left(\frac{u_{i,j}^\nu - u_{i,j-1}^\nu}{h}\right)\right]. \tag{5.14}$$

The resulting fully discretized scheme can then be written as

$$\begin{aligned}(1 + c_1 D_h^2)u_{i,j}^{\nu+1} = \; & (c_2 + c_3 D_h^2)u_{i,j}^\nu + (c_4 + c_5 D_h^2)u_{i,j}^{\nu-1} \\ & + \delta t^2\{\sigma_{1_{i,j}}^\nu + \sigma_{2_{i,j}}^\nu\},\end{aligned} \tag{5.15}$$

together with the boundary conditions

$$u_{i,j}^{\nu+1} = 0 \;\text{ for } i,j = 0 \text{ or } N, \tag{5.16}$$

where $c_1 = -\mu\delta t/h^2$, $c_2 = 2$, $c_3 = (\delta t - \mu)\delta t/h^2$, $c_4 = -1$ and $c_5 = 0$. Other choices of time discretization lead to expressions of the same form in (5.15). For example, approximating the viscoelastic damping by the Crank–Nicolson method (WOOD [1990]), instead of the implicit Euler method (5.3), corresponds to

$$\mu\triangle u_t \approx \mu(\triangle u^{\nu+1} - \triangle u^{\nu-1})/2\delta t \tag{5.17}$$

and a finite difference scheme of the form (5.15) with $c_1 = -\mu\delta t/(2h^2)$, $c_2 = 2$, $c_3 = (\delta t/h)^2$, $c_4 = -1$ and $c_5 = -\mu\delta t/(2h^2)$. Similarly, the explicit forward Euler approximation

$$\mu\triangle u_t \approx \mu(\triangle u^{\nu} - \triangle u^{\nu-1})/\delta t \tag{5.18}$$

is given by $c_1 = 0$, $c_2 = 2$, $c_3 = (\delta t + \mu)\delta t/h^2$, $c_4 = -1$ and $c_5 = \mu\delta t/h^2$.

The fully discretized version of the first time step (5.8) has a similar form. The timestepping was implemented in the following adaptive fashion. We started with a small time step ($\delta t = 10^{-6}$ for the 200×200 mesh used in §6) to accurately capture the initial rapid selection of large scale structures, and then slowly increased the time step as the evolution

process slows down. More precisely, after each 100 time steps the maximum wavespeed c of the associated (locally) linearized undamped problem was estimated, and the time step then doubled provided that an overly conservative CFL–condition was satisfied (we used the criterium $h/\delta t < 50c$ for the numerical examples in §6). This continued until some preset maximum time step was reached (chosen as 10^{-3} for the examples presented below).

Solving the linear system at each time step is equivalent to inverting a highly structured, banded, symmetric $(N-1)^2 \times (N-1)^2$ matrix. This sparseness and symmetry was exploited by storing the matrix in an upper packed band storage mode. At each time step ν, solution of the linear system (to obtain $u_{i,j}^{\nu+1}$) was accomplished in an iterative fashion, using a vectorized conjugate gradient method with incomplete Cholesky factorization as the preconditioner (the relative residual error tolerance was chosen as 10^{-12}) as implemented in the subroutine DSDCG from the Engineering and Scientific Subroutine Library (ESSL Release 5, IBM).

The algorithm was implemented in vectorized form on the IBM 3090–600 J of the Cornell National Supercomputer Facility. The results of several numerical experiments are presented and discussed in §6. To the best of our knowledge these constitute the first numerical simulations of an anisotropic time–dependent anti–plane shear problem that can undergo phase changes.

6 Numerical Results

6.1 Introduction

We now present some numerical simulations of the dynamical evolution of patterns and microstructure in both the isotropic and anisotropic anti–plane shear problems described in §2, using the finite difference algorithm described in §5.

The dynamical creation of microstructure raises some interesting numerical issues. The

results of any numerical model (of a continuum phenomenon) which may eventually display structures on the scale of the mesh have to be interpreted with great care. As in the numerical examples presented below, this numerical manifestation of complicated equilibria (or asymptotic solutions) also rears its head in the related investigations in SILLING [1988a], COLLINS & LUSKIN [1989], BALL et al. [1991] and HOLMES & SWART [1991], as well as in numerical problems of engineering concern in, for example, viscoplasticity, turbulence and optimal design. Even when regularizing terms, such as those corresponding to viscosity, capillarity or temperature effects, are included in the corresponding analytical models — thereby forcing all solutions to converge to one of a finite (but possibly large) number of equilibrium solutions — such equilibrium solutions can still contain sufficiently small structures so as to render the full numerical resolution of the smaller scales impractical.

One possible solution to this dilemma is to interpret the numerical and analytical models as different but related dynamical systems in order to determine the conditions which will imply a *gradual* numerical refinement and to estimate the rate of this refinement. This would motivate the current belief that, over sufficiently short periods of time and before the finite dimensional barrier has had a severe effect, the numerical solution of the "truncated system" will provide an accurate description of the real solution. A motivating example is provided by the remarkable accuracy with which the asymptotics of a "nonlocal" model of BALL et al. [1991] are followed, for finite times, by a numerical solution based on a finite number of Fourier modes (see §5–§6 of BALL et al. [1991]). The modal asymptotics allow one to predict a "crossover" time beyond which the numerical solution and the true solution seperate. Unfortunately, such detailed estimates are not available for the anti-plane shear problement problem.

For all the simulations described here we used a 200×200 mesh on the square domain $\Omega \equiv (0,1) \times (0,1)$. This resolution quickly became insufficient as fine structure appeared (especially at the boundary) and generally runs were terminated at the stage when spatial

wavelengths of the order of three times the mesh size started to appear. After starting with a time step of 10^{-6}, adaptive timestepping was implemented, as described in §5, so as to allow the gradual increase (when permitted) to a maximum time step of 10^{-3}. In the numerical examples shown below, the specific form of the stress–strain response σ was chosen to display interesting and revealing behavior of the anti–plane shear problem, and an appropriate value for μ was then experimentally determined so as to ensure that all the examples evolve at roughly the same rate. In this respect, note that the equation of interest (2.13) is invariant under the transformation

$$(t, \sigma, \mu) \mapsto (\frac{t}{T}, T^2\sigma, T\mu), \tag{6.1}$$

which provides a basis for comparing different choices of μ.

It should be noted that the particular stress–strain response functions σ chosen in the numerical examples all fail to be globally Lipschitz continuous (see Theorem 3.1). However, in the context of the numerical solutions, we observe that ∇u and u_t are uniformly bounded (in L^∞) over the period of numerical integration, and that there is no numerical evidence of the development of singularities in ∇u. This implies that we can consider σ to be modified outside a region of compact support so as to be globally Lipschitz.

The figures in this section were generated by draping a lower resolution (100×100) wireframe over the data set (without smoothing). This low resolution obviously causes some aliasing effects, thereby limiting the interpretation of some of the finer patterns. This is particularly severe in the top view of Figure 16. A more revealing visualization of some of these results was achieved by using the Wavefront animation package, and resulted in a rather insightful video animation (SWART & HOLMES [1991]).

6.2 An Isotropic One–Valley Material

As our first example we consider the constitutive law $\sigma : \nabla u \to g(|\nabla u|^2)\nabla u$ for the isotropic anti–plane shear problem (2.13)–(2.15). The associated local elastic energy function $W =$

$W(|\nabla u|)$ is chosen with a strict local minimum (in the variable $|\nabla u|$) at $|\nabla u| = \gamma_0 > 0$; i.e. convexity of W fails rather severely due to the continuum of minima lying along a circular valley (at a distance γ_0 from the undeformed state) in strain space. Minimization of $\int_\Omega W(|\nabla u|)\,\mathbf{dx}$ (which requires $|\nabla u| = \gamma_0$ a.e.) under the constraint of the boundary condition $u = 0$ on $\partial\Omega$ can be achieved by any member of the large class of absolute minimizers constructed as in Theorem 2.3 (cf. Remark 5 following the theorem). An interesting question is whether the dynamical route to minimization will be achieved by a relatively uniform mixture of a continuum of phases, or whether only a few of the minima of W will be explored.

To illustrate this phenomenon, we chose a viscoelastic damping of $\mu = 0.25$ and $\gamma_0 = 1$ with $W(|\nabla u|) = \frac{1}{4}(|\nabla u|^2 - 1)^2$, giving $\sigma(\nabla u) = (|\nabla u|^2 - 1)\nabla u$. The anti-plane shear problem (2.13)–(2.15) was then solved with initial displacement $u(x, y, 0) = x^2(x-1)y(y-1)$ and zero initial velocity $u_t(x, y, 0) = 0$. Figures 6–9 respectively show the solution (displayed at a 100×100 resolution) at times $t = 0.0$, 0.5, 1.0 and 2.75. The decay in energy is shown in Figure 10. We point out its similarity with the energy decay presented in FRENCH & WAHLBIN [1991, Figure 4.2] for a different but related isotropic problem.

The asymmetrical initial data leads to formation of an off–center (in x) displacement ridge. This forces the creation of further ridges, as the displacement field adjusts itself in an attempt to satisfy $|\nabla u| = 1$. The "large scale" structure visible at $t = 0.5$ (Figure 7), which is strongly influenced by initial data, forms during the early rapid energy decay and is essentially complete once the kinetic energy begins its monotonic decay (Figure 10). Once the gross structure is established, it undergoes little change: in particular, the "ridges" — regions of rapid change in $|\nabla u|$ — do not move. The peak ridge buckles around $t = 1.0$ (Figure 8) and a limited amount of fine structure appears to grow from the diagonal ridges (visible at $t = 2.75$, Figure 9). Note that all of this fine structure appears after the kinetic energy has begun its monotonic decay ($t > 0.7$), and, indeed, only after the kinetic energy

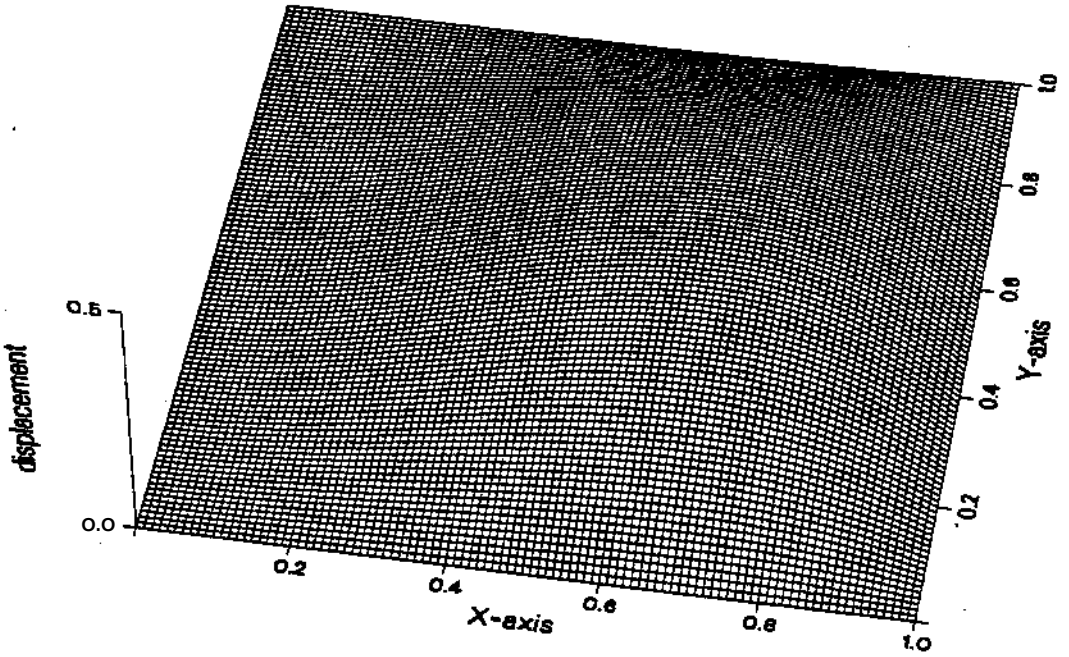

Figure 6: Numerical solution at t = 0.0 (initial data) for the first isotropic anti-plane shear example, as described in §6,2.

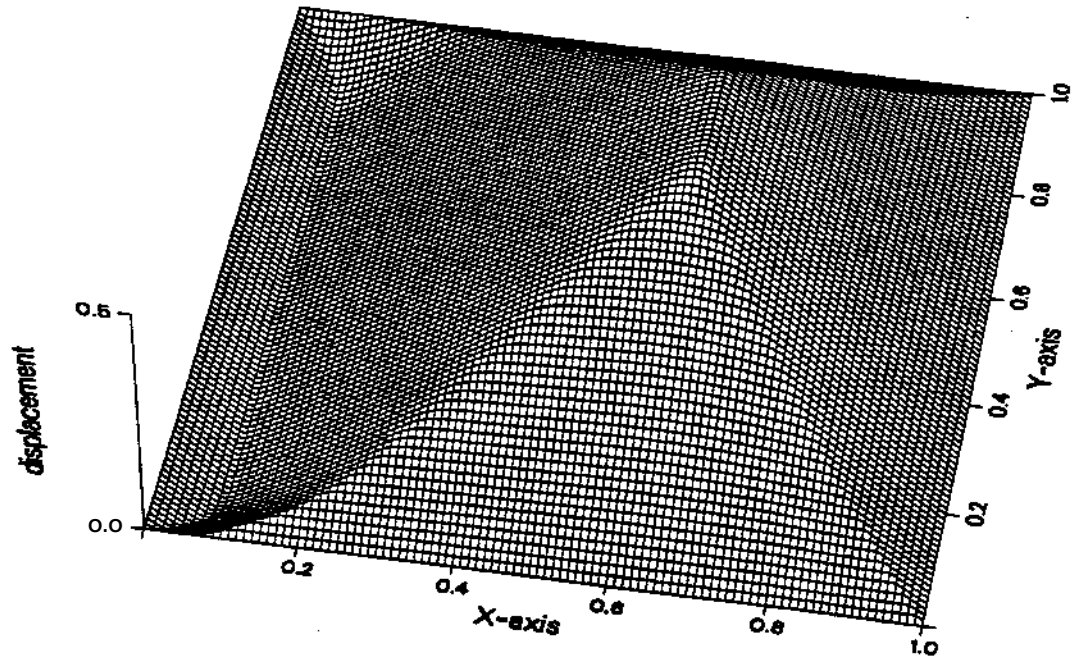

Figure 7: Solution at t = 0.5 for the first isotropic problem, as described in §6.2.

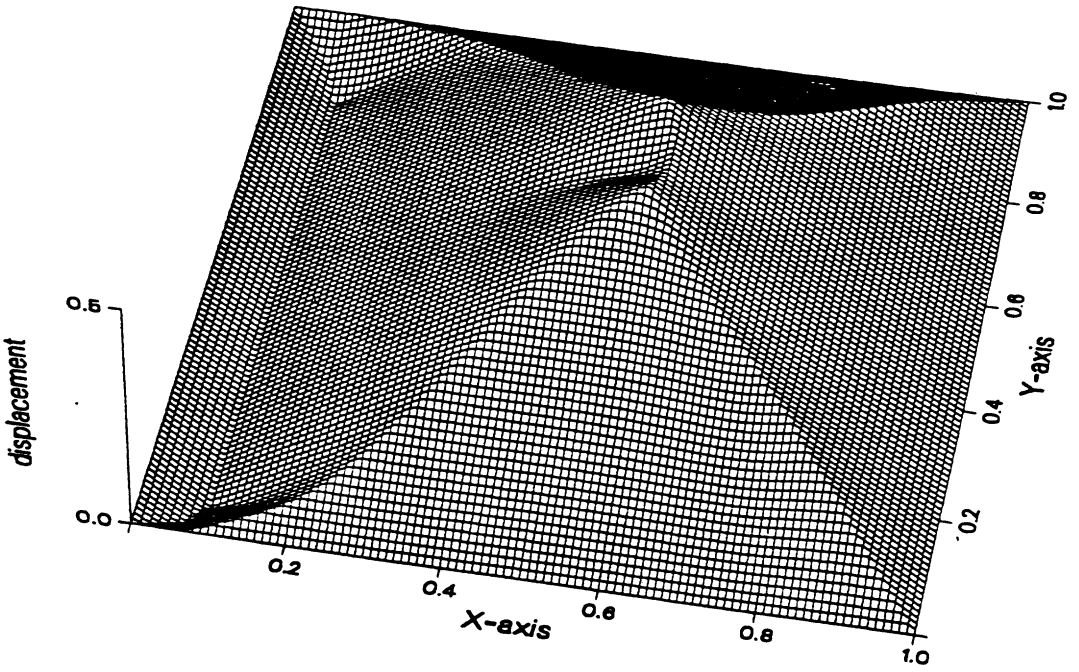

Figure 8: Solution at $t = 1.0$ for the first isotropic problem, as described in §6.2.

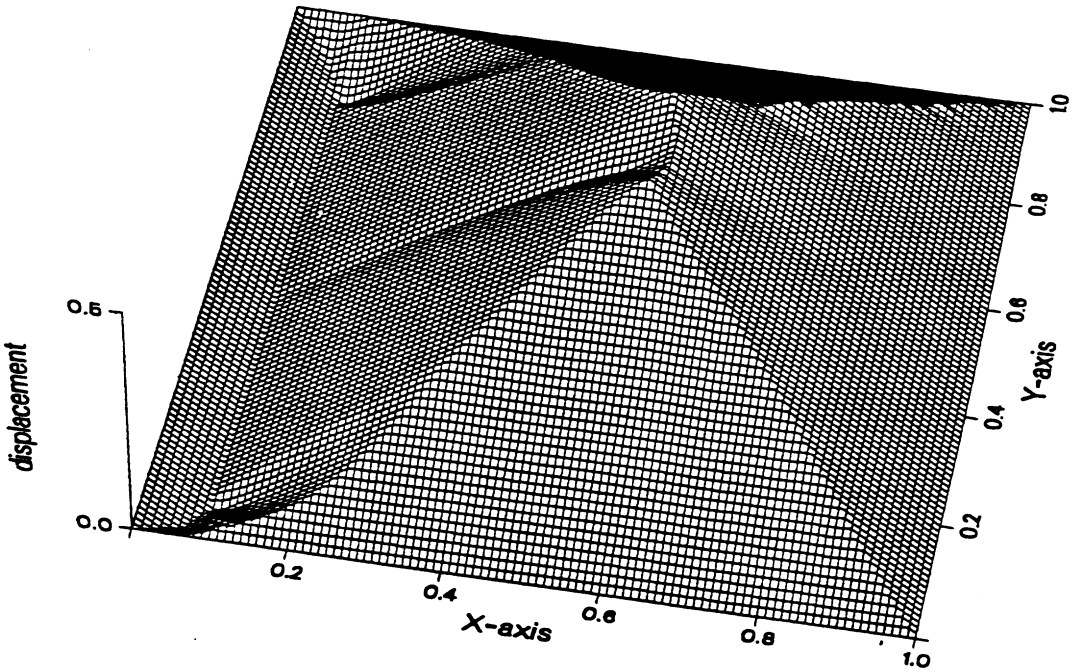

Figure 9: Solution at $t = 2.75$ for the first isotropic problem, as described in §6.2.

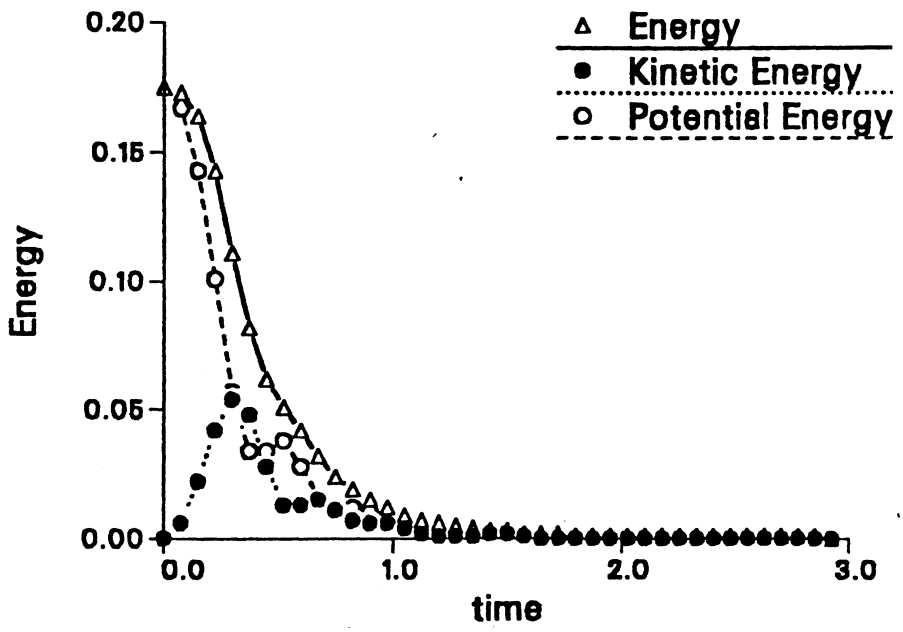

Figure 10: Energy decay for the first isotropic problem, as described in §6.2.

is practically zero. Relatively few "large" phase domains form, and, aside from the fine structure, only 5 or 6 points on the circle $|\nabla u| = 1$ are represented at $t = 2.75$. By this time the total energy has essentially decayed to zero, suggesting that minimization is almost achieved. Once sharp phase boundaries — near discontinuities in $|\nabla u|$ – have formed (Figure 8) they seem unable to propagate transversely. We note that the reflectional symmetry of the initial data about $y = 0.5$ is preserved, although the graphical visualization of Figure 9 obscures this fact. The "fine structure" valleys branching from the nearest diagonal ridge are not visible from the view shown: rotation of the image reveals the symmetry. Many of these general features will reappear in the computations described below, including those with anisotropic constitutive laws. We summarize the key features:

(1) Rapid initial energy decay and "set in" of gross large scale features.

(2) Formation of sharp boundaries between phases and apparent inability of these boundaries to propagate transverse to their orientation.

(3) Slow growth of fine structure in regions where ∇u is not in equilibrium.

6.3 An Isotropic One–Well One–Valley Material

In this example we again use an isotropic constitutive law (as in §6.2), but with a local elastic potential function $W = W(|\nabla u|)$ which possesses two separated local minima at $|\nabla u| = 0$ and $|\nabla u| = \gamma_0$. In particular, we chose $W(\gamma) = 4\gamma^2(\gamma - \gamma_0)^2$, which gives $\sigma(\nabla u) = 16(|\nabla u| - \gamma_0)((|\nabla u| - \gamma_0/2)\nabla u$. Here we used $\gamma_0 = 1$. We solved the dynamical anti–plane shear problem with $\mu = 0.5$, and initial data $u(x, y, 0) = .05 \sin 5\pi x \sin 3\pi y$ and $u_t(x, y, 0) = 0$. Figures 11 and 12 respectively show the solution (displayed at a 100×100 resolution) at $t = 0.0$ and 1.4. The decay in energy is similar to that of the previous example in §6.2, and is not shown here.

The initial dynamical selection of a few "large" phase domains is similar to (although more rapid than) that of the first isotropic example (described above in §6.3). In this case the additional freedom made possible by a larger number of accessible phases allows the basic discrete symmetry of the initial conditions to be preserved. There is no evidence of fine structure.

As in the previous isotropic example, highly curved phase boundaries appear to be dynamically unstable. Although it is not readily apparent from the visualization of the solution at $t = 1.4$ (Figure 12), a high resolution view reveals piecewise almost–constant gradients at this stage.

In both this and the previous isotropic problem energy appears to approach its absolute minimum. We observe that classical minimizers involving only finitely many domains can be easily constructed in these cases: one need merely pick piecewise constant ∇u to form large pyramids or "rooftops".

6.4 An Anisotropic Two–Well Material

We henceforth concentrate on solutions of the anti–plane shear problem (2.13)–(2.15) with the anisotropic constitutive law $\sigma(\nabla u) = (\sigma_1(u_x), \sigma_2(u_y))$, introduced in §2.2 and associated

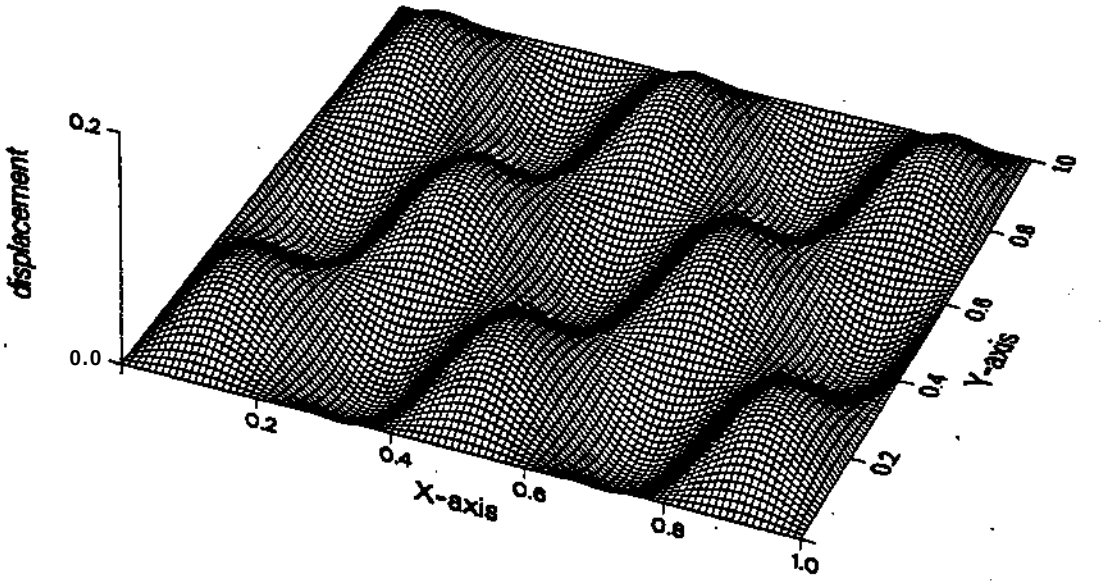

Figure 11: Numerical solution at.i = 0.0 (initial data) for the second isotropic anti-plane shear problem, as described in §6.3.

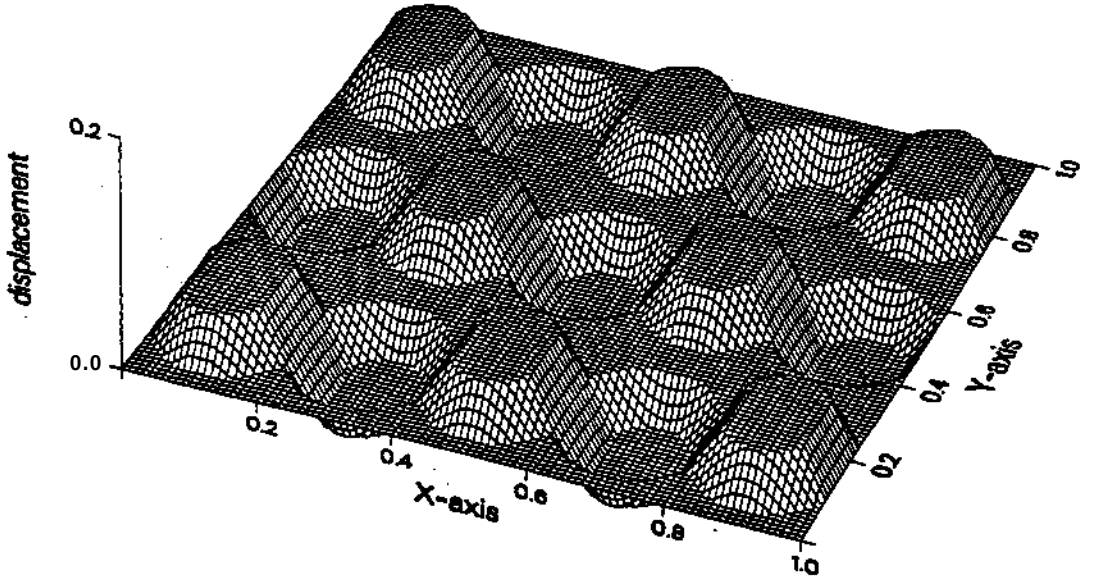

Figure 12: Solution at t = 1.4 for the second isotropic problem, as described in §6.3.

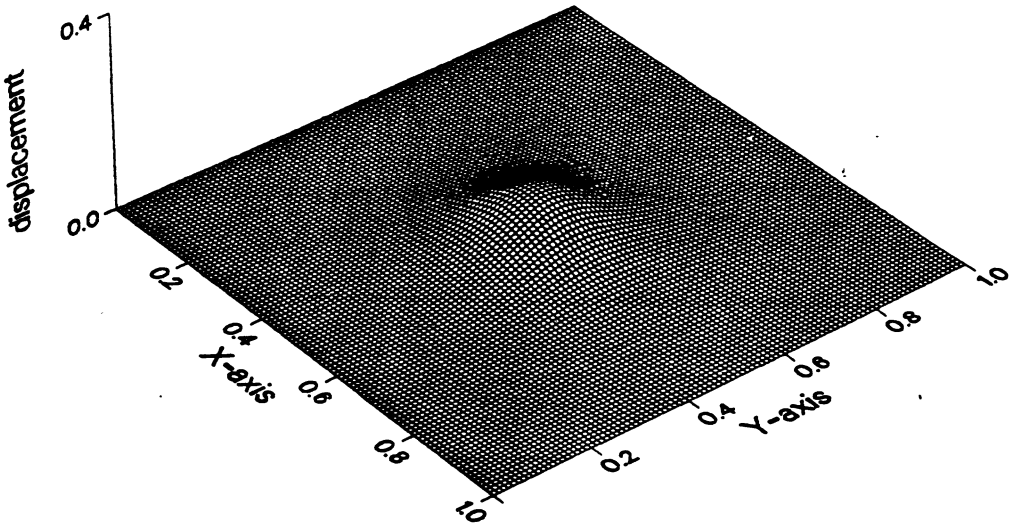

Figure 13: Numerical solution at $t = 0.0$ (initial data) for the two–well anisotropic problem described in §6.4.

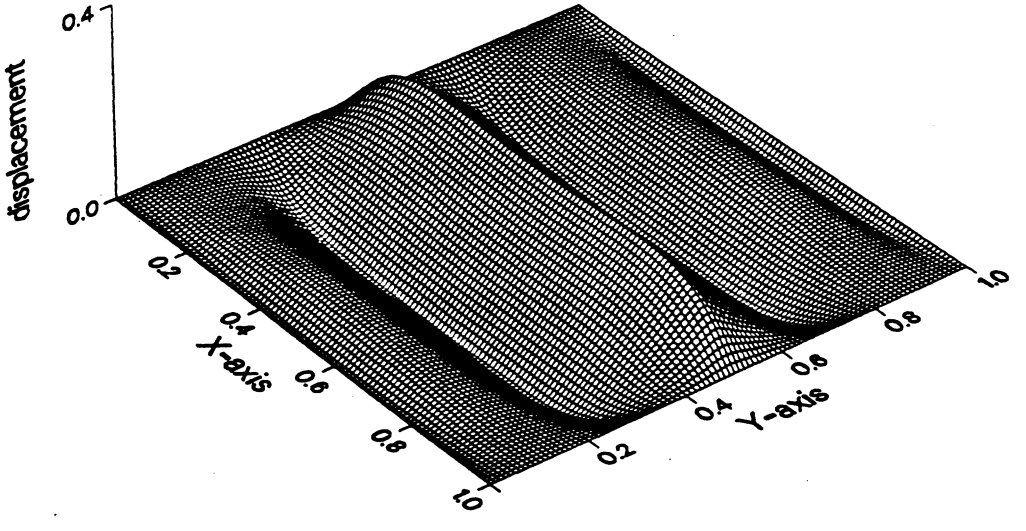

Figure 14: Solution at $t = 0.5$ for the two–well anisotropic problem, as described in §6.4.

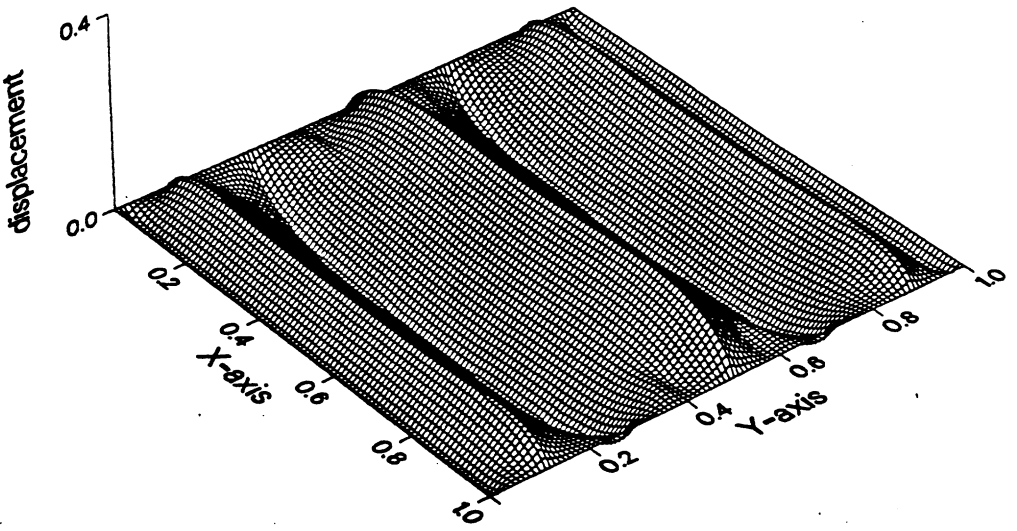

Figure 15: Solution at $t = 1.0$ for the two–well anisotropic problem, as described in §6.4.

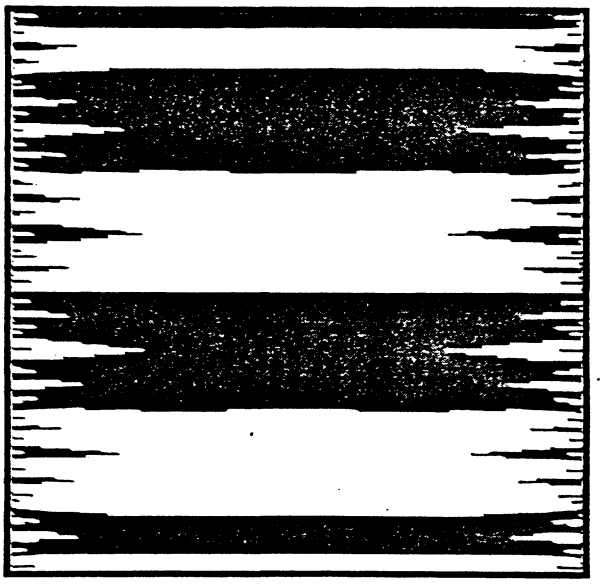

Figure 16: Solution at $t = 4.0$ for the two–well anisotropic problem: top view, $u_y \approx +1$, white; $u_y \approx -1$, black. Jaggedness of phase boundaries largely due to visualization process.

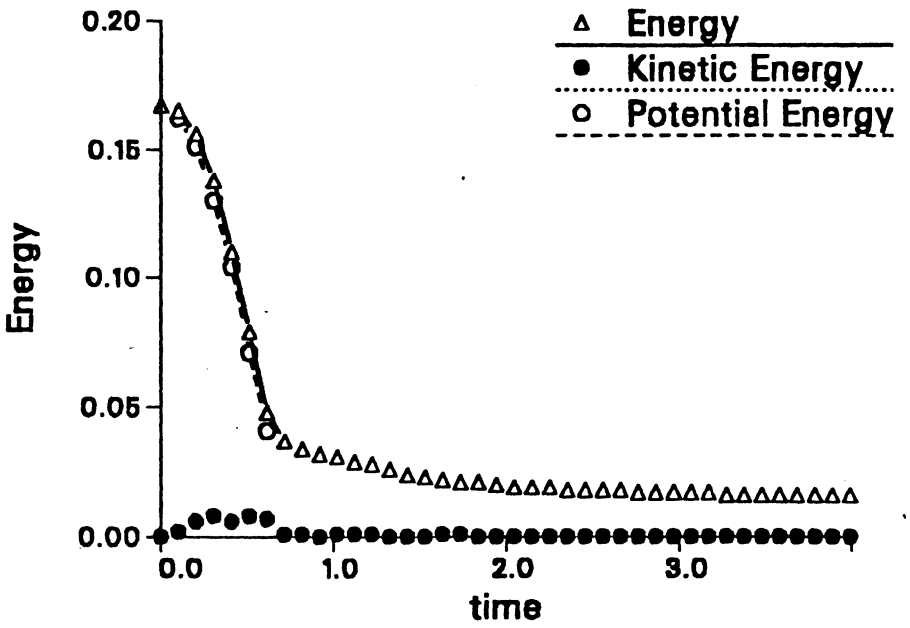

Figure 17: Energy decay for the two–well anisotropic problem, as described in §6.4.

with cubic symmetry, and its effect on the dynamical evolution of solutions. As our first example, we take $\sigma_1(u_x) = u_x$ and $\sigma_2(u_y) = u_y^3 - u_y$ and numerically solve the resulting anti–plane shear problem with $\mu = 0.05$:

$$u_{tt} = u_{xx} + (u_y^3 - u_y)_y + 0.05\Delta u_t \quad \text{on} \quad (0,1) \times (0,1). \tag{6.2}$$

Note that the corresponding local stored elastic energy $W(\nabla u) = \frac{1}{2}u_x^2 + \frac{1}{4}(u_y^2 - 1)^2$ has two isolated wells at $(u_x, u_y) = (0, \pm 1)$ and therefore, by Theorem 2.3, possesses no absolute minimizer of the energy. Here the boundary conditions interact with the constitutive law to force candidates for absolute minimizers to exhibit refinement *throughout* the domain.

We used as initial displacement

$$u(x,y,0) = \frac{1}{10}\text{sech}\left(10\sqrt{(x-\tfrac{1}{2})^2 + (y-\tfrac{1}{2})^2}\right)\sin \pi x \sin \pi y, \tag{6.3}$$

which corresponds to a smooth bump in the center of the unit square, and the initial velocity was again taken to be zero. Figures 13–16 show how increasingly finer ridges develop parallel

to the x–axis in an effort to minimize the total energy. However, the refinement process slows down and relatively large single phase domains survive for long times. The resulting energy decay is shown in Figure 17. Note that the energy does not appear to be decaying to zero (the global minimum).

In Figures 13–16 one initially observes an essentially "linear" wave propagation forming large ridges in the x direction, together with an associated rapid rise and fall of kinetic energy, which is shown in Figure 17. This continues until the ends of the ridges reach the boundary at $x = 0, 1$. The incompatibility at the boundary manifests itself in large, local concentrations in the potential energy — chiefly along the boundary and between the now well–established ridges, thereby initiating the slow inward growth of parallel whiskers. Note that, once formed, the ridges do not move (although the video animation of this numerical run shows a slow but steadily decaying global vertical oscillation) and that the discontinuities in u_y do not propagate in the transverse direction.

The pattern achieved at $t = 4.0$, with increasingly fine whiskers invading the interior region of large ridges from the boundaries $x = 0, 1$, is strongly reminiscent of the sketch provided in Figure 23 of BASINSKI & CHRISTIAN [1954], showing a cross section of a cubic (austenite) to tetragonal (martensite) interface observed in indium–thallium alloys. They remark that "fine scale twinning is necessary to prevent large strain energy at the interface, but is obviously unfavourable energetically in the more remote regions of the tetragonal phase". There are at least two important differences in the situations. BASINSKI and CHRISTIAN evidently assumes an energy penalty associated with strain jumps, whereas our effects are dynamical. Moreover, they are dealing with an internal phase boundary in a three–dimensional geometry, on which the rank–1 condition (2.19) is not met (BALL & JAMES [1987]); this is replaced in our two–dimensional calculation by incompatibility at the boundary. Nonetheless, we feel that the dynamical origin of the whiskers, as the system either fails to minimize or does so extremely slowly, provides another mechanism

for interface accomodation in addition to explicit surface energy penalties. We comment further in §7.

We also note that KOHN & MÜLLER [1992] construct a two-dimensional scalar field exhibiting self similar twin refinement much like that of Figure 16 near a martensite/austenite boundary. Their analysis involves minimization of an elastic energy similar to the two-well potential of this system, augmented by the term nu_{yy}^2 which penalizes large strain gradients.

The growth of fine structure is very slow, occuring after t = 1.0, when the kinetic energy is essentially zero (Figure 17) and leads to only modest reduction in potential energy. This is in sharp contrast to the computations described earlier and below, for problems in which absolute minimizers do exist; it suggests that in problems with no such minimizers the dynamics may not minimize energy. In this respect Figure 17 should be compared with the corresponding Figure 2 for a one-dimensional problem which is known not to minimize energy. Noting that Figure 17 only includes the first 13% of the comparable time range shown on Figure 2, it is plausible that the solution is approaching a non-minimizing state.

We finally remark that the initial burst observed in kinetic energy — during which the larger ridges set in — followed by the period of slow decay of energy — during which we observe the growth of microstructure — is a common feature in all the anisotropic examples presented here, as it was for the first of the isotropic examples above.

6*5 An Anisotropic Four-Well Material

As in §6.4, we consider the anisotropic constitutive law $a(Vu) = (<T\backslash(u_x), a2(u_y))$. We now choose $oi(u_x) = a\{u_x + 0.4)$ and $o_2\{u_y) = a(u_y)$, with $a(j) = 7^3 - 7$ and /1 = 0.025, resulting in the equation:

$$u_{tt} = a(u_x + 0.4)_x + a(u_y)_y + 0.025\text{Au}^* \quad \text{on} \quad (0,1)\text{x}(0,1). \tag{6.4}$$

The corresponding local stored elastic energy is given by $W(Vu) = \backslash\{\{u_x + 0.4)^2 - \text{I})^2 + \text{J}(u_y^2\text{-l})^2$ and has four isolated potential wells at (u_x, u_y) = (-1.4, ±1) and (0.6, ±1), where

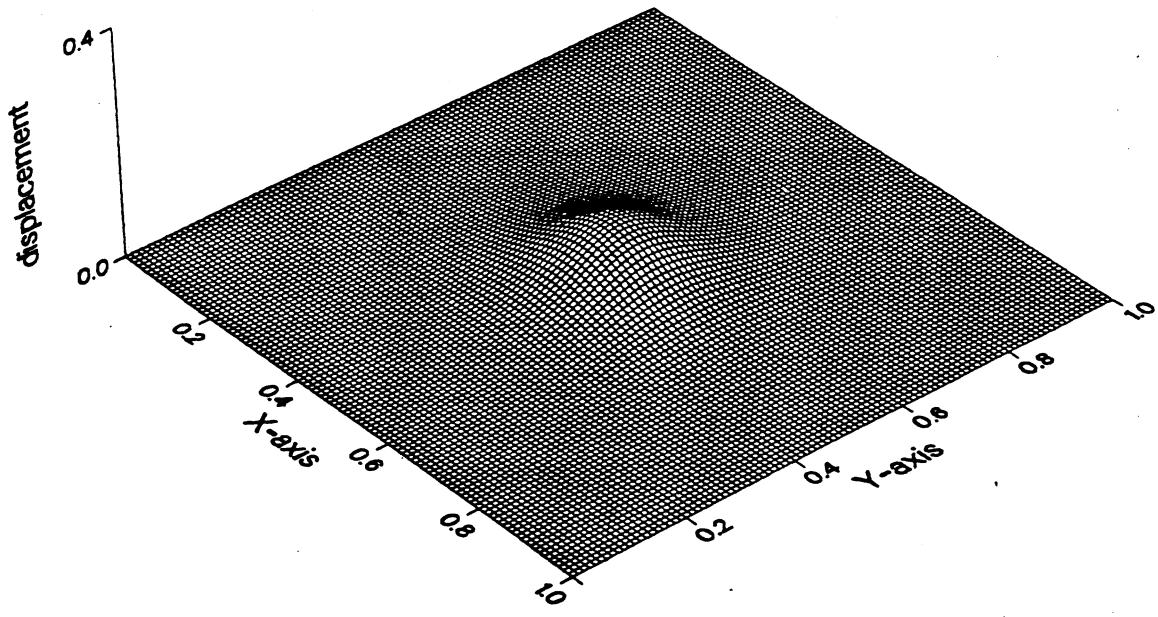

Figure 18: Numerical solution at $t = 0.0$ (initial data) for the four–well anisotropic problem described in §6.5.

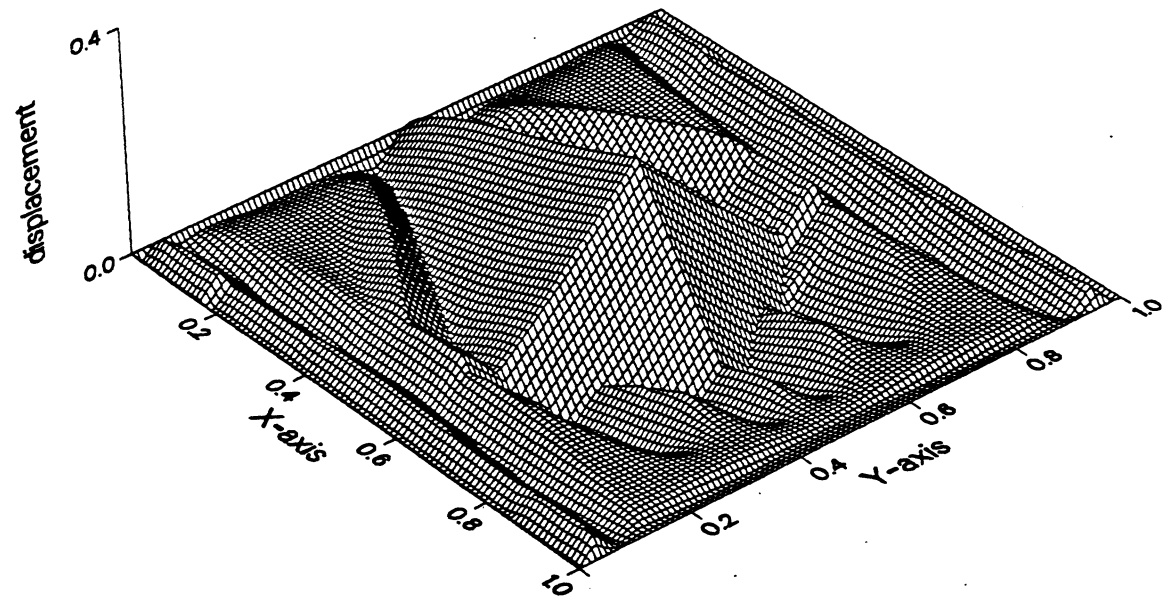

Figure 19: Solution at $t = 0.5$ for the four–well anisotropic problem, as described in §6.5.

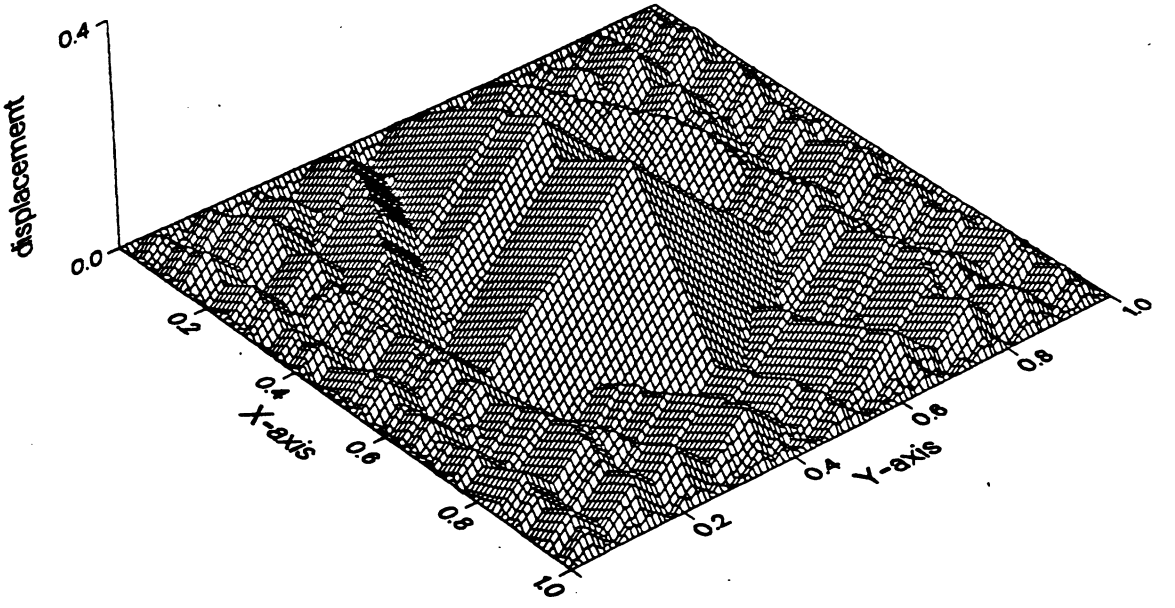

Figure 20: Solution at $t = 3.3$ for the four-well anisotropic problem, as described in §6.5.

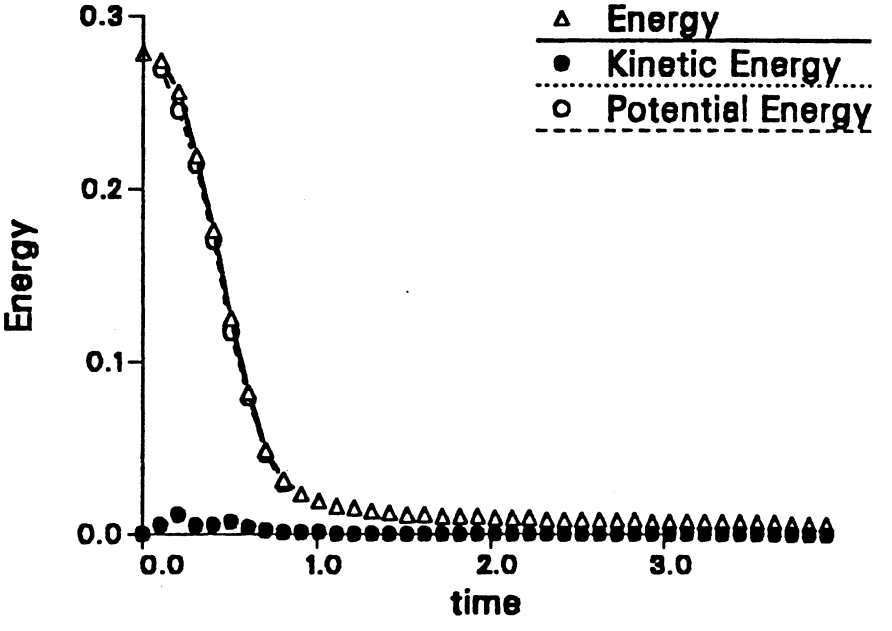

Figure 21: Energy decay for the four–well anisotropic problem, as described in §6.5.

$\phi = 0$. As initial data we used the smooth bump displacement of equation (6.3) together with zero initial velocity. Although there are enough wells to form classical minimizers (Theorem 2.3), for piecewise homogeneous displacements the four phases corresponding to the four isolated potential wells can also meet together in, for example, skewed pyramids. As such structures cannot tile the square, we expect to observe refinement at the boundary. This process is illustrated in Figures 18–20 which respectively show the numerical solutions at $t = 0.0$, 0.5 and 3.3. The energy decay is shown in Figure 21, but note that here, in contrast to the previous two–well material, energy appears to be approaching its minimum.

Initially, the solution is characterized by the rapid "setting in" of the large pyramid (see Figure 19) — whose central peak is derived from the initial state — with subsequent structures attempting to fit around this pyramid. The shape of this pyramid, which is uniquely determined by the location of the four potential wells in this example, is incompatible with the domain, with the result that the pyramid's back is bent at $t = 0.5$ and broken at $t = 1.0$. Ridges are also observed to form initially near $y = 0$ and 1, but are rapidly broken into chains of pyramids. The higher resolution achieved in the associated video animation of this refinement process indicates that the asymptotic state also contains fine structure in the interior, which, if true, is probably due to the inability of the chains of pyramids to completely "tile" around the large pyramid. This raises the possibility that, even when absolute minimizers of the type constructed in Theorem 2.3 are available, they may not be accessible for all initial data. However, in contrast to the two–well case, at $t = 4.0$ the energy is essentially zero (Figure 21), indicating that a minimum may be achieved.

6.6 An Anisotropic Nine–Well Material

As in §6.4 and §6.5 above, we consider the anisotropic constitutive law $\sigma(\nabla u) = (\sigma_1(u_x), \sigma_2(u_y))$. Here we choose $\sigma_1(u_x) = \sigma(u_x + 0.7)$ and $\sigma_2(u_y) = \sigma(u_y + 0.7)$, with $\sigma(\gamma) = \gamma(\gamma^2 - 4)(\gamma^2 -$

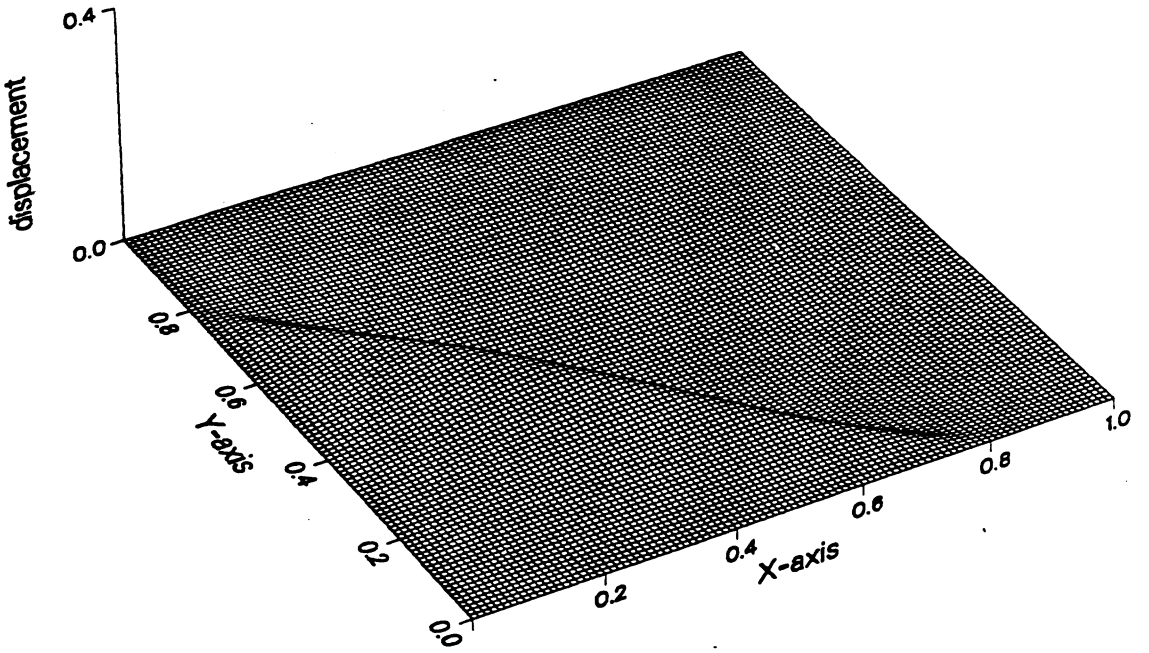

Figure 22: Numerical solution at $t = 0.0$ (initial data) for the nine–well anisotropic problem described in §6.6.

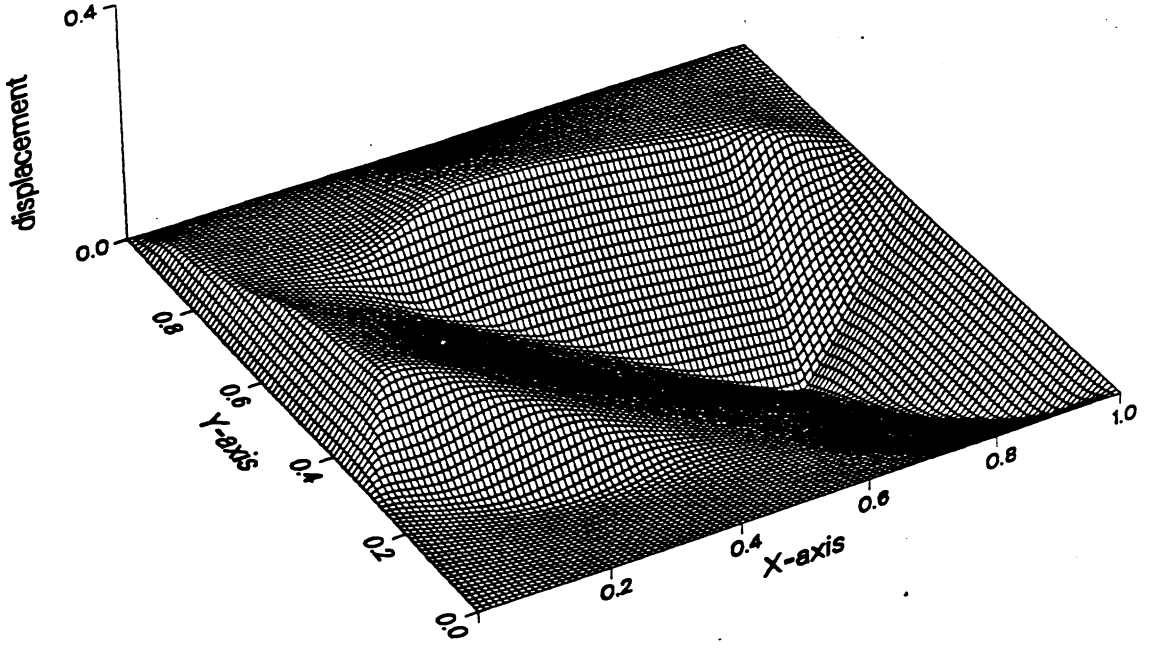

Figure 23: Solution at $t = 0.5$ for the nine–well anisotropic problem, as described in §6.6.

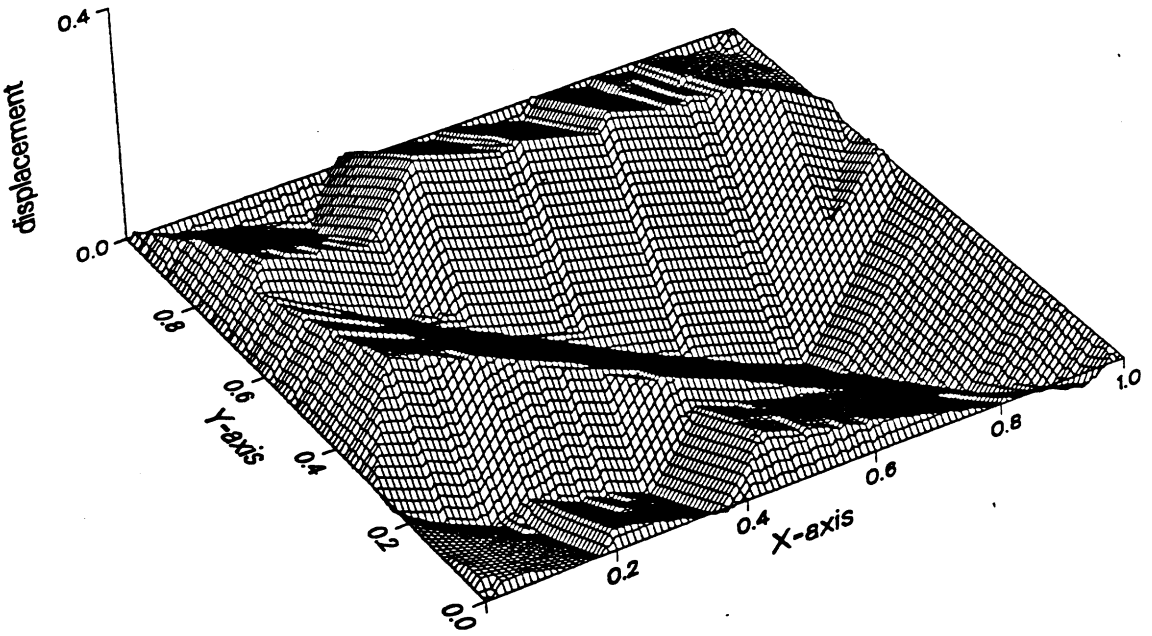

Figure 24: Solution at $t = 3.2$ for the nine–well anisotropic problem, as described in §6.6.

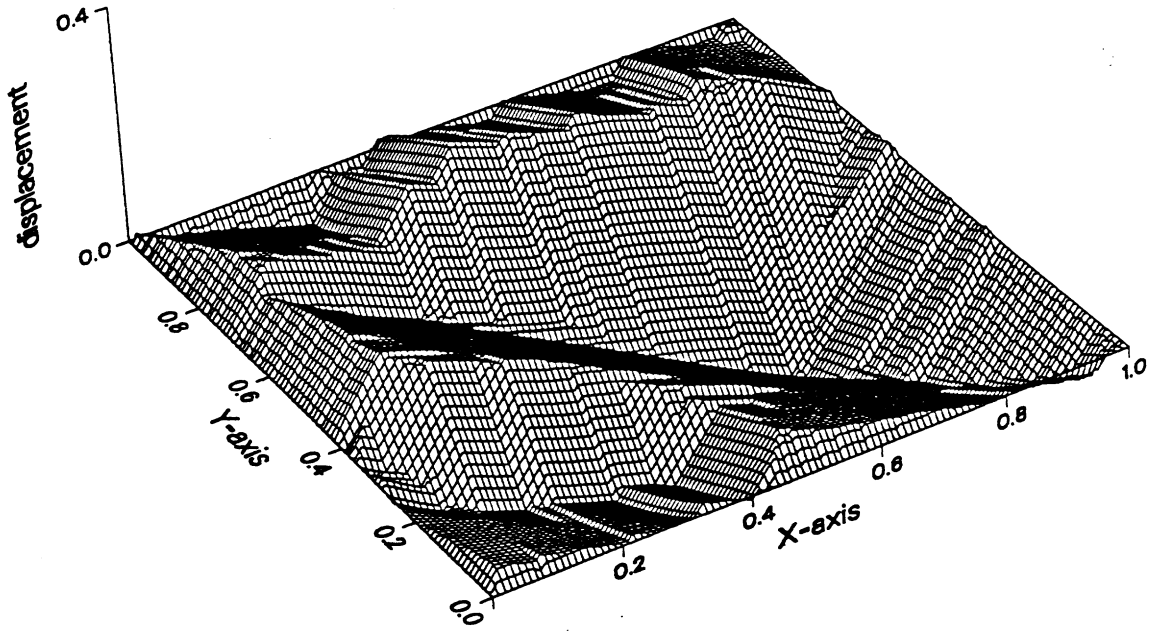

Figure 25: Numerical solution at $t = 3.2$ for the nine–well anisotropic problem with slightly perturbed initial data as described in §6.6.

4/3) and $ft = 0.25$, resulting in the equation:

$$u_{tt} = 0(ux + 0.7)_x + c(u_y + 0.7)_y + 0.25Au_t \quad \text{on} \quad (0,1)x(0,1). \tag{6.5}$$

The corresponding local stored elastic energy is given by

$$W(V\text{«}) = \underset{o}{Ul(\tilde{u_x} - 2)^2(t2_I + 2)^2} + \underset{o}{Ul(\tilde{u_y} - 2)^2(\text{«}_v + 2)^2}, \tag{6.6}$$

with $(\tilde{u}_x = u_x + 0.7, \dot{ii}_y = Uy + 0.7)$, and has nine isolated wells where $W = 0$. As initial data we used

$$u(z, y, 0) = -\frac{1}{20}\tanh(40(x + y - 0.8) + 1 - 2y)\sin irx \sin Try, \tag{6.7}$$

$$u_t = 0,$$

which forms an asymmetric ridge (shown in Figure 22) at $t = 0$. Figures 22-24 respectively show the numeria! solutions (using a 100 x 100 resolution) at $t = 0.0$, 0.5 and 3.2. The energy decay is not shown but is similar to that of the four-well material of §6.5, with the energy apparently decaying to its minimum.

The presence of more potential wells (nine in this case) implies more freedom in accomodating incompatibility at the boundary than in the previous example, with the result that fine structure is only seen "near" the boundary. In this example, part of the initial condition (the steep part of the ridge in Figure 22) lies in the high strain well at $(u_x, u_y) = (-2.7, —2.7)$, and appears to be "pulled out" of this well by the dynamics, as we do not observe any regions in this phase at $t = 3.2$.

We conclude with an example displaying the subtle dependence of the solution on initial conditions. This property is even more striking in the two-dimensional anti-plane shear problem than in the one-dimensional models of BALL et al. [1991]. In Figure 25 we show the solution at $t = 3.2$ of the above nine-well problem with a slightly perturbed initial condition. We solved (6.5) with identical numerical procedures, but added the small sinusoidal

perturbation given by $0.0001 \sin 10\pi x \sin 10\pi y$ to the initial data (6.7). The inital selection of large scale features as well as the manner in which energy decays are almost identical to that of the unperturbed problem. However, when comparing Figure 25 with Figure 24, we notice a markedly different distribution of the smaller scales. The construction in the proof of Theorem 2.3 shows that this problem, like the one–dimensional model (2.6), possesses a continuum of equilibria, which are now, unlike that case, all absolute minimizers. It is thus reasonable to expect solutions started on an arbitrary arc of initial data to all approach distinct equilibria in which the fine phases are packed in different fashions near the boundaries. This is what we appear to see in Figures 24–25.

7 Conclusions

The models described and analyzed in this paper were designed to provide insight into the dynamical formation of microstructure in elastic crystals. Our contributions are in four areas: (1) characterization of non–convex stored energy functions for anti–plane shear problems in terms of their failure or ability to admit absolute minimizers; (2) proof of existence–uniqueness theorems for certain two dimensional mathematical models of non-linear viscoelasticity, and partial results characterizing the ability or lack thereof of such models to minimize energy and the manner in which this occurs; (3) development of algorithms for the numerical solution of the model problems; (4) numerical simulation of several specific models and assessment of these results in the light of the (incomplete) theory.

The choice and study in BALL et al. [1991] of three one–dimensional models displaying the eventual creation of fine structure, provided several new insights and also motivated and guided our subsequent study of the two–dimensional anti–plane shear problem. Noting the inability of one–dimensional models to describe the complicated microstructure and geometric patterns observed in certain crystals, but not wishing to tackle the formidable

three–dimensional problem directly, we formulated and studied the two–dimensional problem of dynamical anti–plane shear with linear viscoelastic dissipation. Both isotropic and anisotropic constitutive laws, which can allow multiple phases, were considered. The ability of such laws to deliver minimizing sequences and minimizers for the anti–plane shear problem is described by Theorem 2.3. By employing the change of variables due to RYBKA, the anti–plane shear problem can be transformed into a semilinear degenerate parabolic system, allowing one to establish the existence and uniqueness of solutions (Theorem 3.1) in a similar fashion to that for the one–dimensional problems of BALL et al. [1991]. This nevertheless requires the restrictive assumption that the stress–strain response $\sigma : \nabla u \mapsto \sigma(\nabla u)$ be globally Lipschitz continuous, thereby ruling out constitutive laws possessing more natural growth conditions. Relaxing this restriction requires a more direct exploitation of the geometric properties of σ, which in two and more dimensions proves to be rather difficult, and we discuss some of the complicating but interesting issues surrounding this obstacle, to which we return below. We also discuss the relationship of RYBKA's transformation to the Helmholtz projection and present a more general framework for its derivation.

In §5 we present a finite difference algorithm for the dynamical anti–plane shear problem. The numerical analysis of problems which develop microstructure raises some delicate issues which we discuss in §6.1. The rest of §6 is devoted to numerical simulations of several examples designed to display various aspects of the rich dynamical behavior possible in the anti–plane shear problem and to provide insight into the creation of microstructure for the constitutive laws under consideration.

Our numerical results, together with the analyses of §2 and §3, and the insight gained from the one–dimensional models of BALL et al. [1991] raise the following central issues.

(*a*) *The existence of absolute minimizers as a precondition for energy minimization*

Our numerical experiments suggest the following conjecture: In the absence of an absolute minimizer, there is no solution of the associated dynamical anti–plane shear

problem whose energy achieves the infimum as $t \to \infty$.

In this respect it is insightful to compare the energy decay (Figure 17) of the two–well anisotropic example (which does not possess an absolute minimizer) with the energy decay (Figure 21) of the four–well anisotropic example (which does possess an absolute minimizer). Note that if the above conjecture were true, as in the one–dimensional case (cf. BALL et al. [1991, Theorem 4.1], Theorem 2.1, above), it would provide an additional mechanism to limit fineness, besides the effects of higher strain gradients or interfacial energy penalties. However, see (*e*) below.

(*b*) *Persistence of strain discontinuities*

The numerical experiments of §6 indicate that, as in the one–dimensional case, strain discontinuities can persist without moving into adjacent regions of smooth deformation gradient. Although solutions display slow global oscillations while refining, motion is observed only along and not transverse to interfaces. We do emphasize, however, that this property is special to the linear viscoelastic damping employed in the models of this paper. Other regularization strategies — such as the addition of capillarity effects — may well allow the propagation and (slow) rearrangement of phases.

(*c*) *Sensitive dependence on initial conditions*

This property is even more prominent in the two–dimensional anti–plane shear problem than in the one–dimensional case (see Figures 24 and 25, and the discussion at the end of §6.6). A small change in the initial conditions or constitutive model delivers almost indistinguishable solutions and decay of energy in the short term. However, the distribution of the resulting smaller scales can differ quite significantly. Similarly, small adjustments to the constitutive law deliver markedly different final states.

(*d*) *Refinement at the boundary*

If the phases corresponding to the minimum local stored elastic energy are geometri-

cally incompatible with either the boundary condition and geometry or with the orientation of strain discontinuities present in the initial conditions, then Theorem 2.3 and the second observation above lead one to expect the solution to undergo refinement at these locations in an effort to achieve compatibility in some average microscopic sense. The examples of §6.4, §6.5 and §6.6 provide numerical evidence of this process. Note that internal microstructure due to the incompatibility of different phases is ruled out in the two dimensional anti–plane shear problem, since all phases are automatically rank–1 connected (cf. BALL & JAMES [1987]). However, in certain cases, initial data, geometry, the constitutive law and the apparent persistence of strain discontinuities may conspire to create internal microstructure (Figures 16 and 20).

(*e*) *Extremely slow evolution of fine structure*

It is only after an initial "burst" in kinetic energy (associated with a rapid selection of patterns) and after the kinetic energy has begun its monotonic decay, that microstructure starts to appear. Especially for problems without absolute minimizers, this appears to be an extremely slow process. We remark that this, rather than failure to minimize, may be responsible for the apparent energy plateau reached in Figure 17.

We conclude by remarking on two of the more interesting analytical difficulties encountered in our attempt to exploit the geometrical information inherent in a nonlinear constitutive law. These difficulties deprived this work of what we hoped might lie at its center: a sufficiently strong existence–uniqueness theory for nonlinear constitutive laws and a characterization of the ability or failure of the dynamical anti–plane shear problem to minimize energy.

The first obstacle was the apparent lack of a suitable function space that contains the class of piecewise smooth vector fields and can provide a natural framework within which to analyze the propagation and evolution of strain discontinuities. In retrospect we realized

that this is a problem basic to the study of conservation laws in higher dimensions.

Our second observation is that much of the complexity of the solutions to the transformed problem is due to the presence of the projection operator TIE>, which acts by removing the rotational part of the stress-strain response *a.* In the language of mechanics, this is merely the somewhat obvious observation that, for a conservation law in divergence form, e.g.

$$u_{tt} = diva(Vu) = dii>7T£X7(Vu), \tag{7.1}$$

the dynamics is driven by only a "part" of the nonlinearity <r. In two and higher dimensions, the part of the stress-strain response that is annihilated by the *div* operator, and therefore has no effect in the dynamics, contains all irrotational vector fields (or, in general, tensor fields) — a subspace well-known for its rich behavior (solenoidal vector fields have received the attention of fluid dynamicists for more than a century). An improved understanding of the transformed system, and especially of the behavior of evolution equations of the form

$$Qt = -*_D < T(Q), \tag{7.2}$$

will hopefully provide insight into this mechanism for complexity.

Acknowledgements. Supported by the U.S. Army Research Office under ARO DAAG 29-85-C0018 (Mathematical Sciences Institute), ARO 1-50157 (Center for Nonlinear Analysis) and NSF under DMS 87-03656. The computations were performed using the Cornell National Supercomputer Facility, which receives major funding from NSF and the IBM Corporation, with additional support from New York State and members of the Corporate Research Institute. The authors would like to thank PHOEBUS ROSAKIS and LARS WAHLBIN for encouragement, criticism and for several helpful remarks and references.

References

R. ABEYARATNE & J. K. KNOWLES [1989] Kinetic relations and the propagation of phase

boundaries in solids. *Arch. Rational Mech. Anal.* **114**, 119–154.

R. ABEYARATNE & J. K. KNOWLES [1990] On the driving traction acting on a surface of discontinuity in a continuum. *J. Mech. Phys. Solids* **38**, 345–360.

R. A. ADAMS [1975] *Sobolev Spaces.* Academic Press, New York.

G. ANDREWS [1980] On the existence of solutions to the equation $u_{tt} = u_{xxt} + \sigma(u_x)_x$. *Journal of Differential Equations* **35**, 200–231.

G. ANDREWS & J. M. BALL [1982] Asymptotic behavior and changes in phase in one–dimensional nonlinear viscoelasticity. *Journal of Differential Equations* **44**, 306–341.

S. S. ANTMAN [1983] Coercivity conditions in nonlinear elasticity, in *Systems of Nonlinear Partial Differential Equations* (ed. J. M. Ball), D. Reidel, Dordrecht.

J. M. BALL [1977] Convexity conditions and existence theorems in nonlinear elasticity. *Arch. Rational Mech. Anal.* **63**, 337–403.

J. M. BALL [1990] Dynamics and minimizing sequences, in *Problems Involving Change of Type,* (ed. K. Kirchgässner) Springer Lecture Notes in Physics 359, 3–16, Springer–Verlag, New York, Heidelberg, Berlin.

J. M. BALL, P. J. HOLMES, R. D. JAMES, R. L. PEGO & P. J. SWART [1991] On the dynamics of fine structure. *J. Nonlinear Science* **1**, 17–70.

J. M. BALL & R. D. JAMES [1987] Fine phase mixtures as minimizers of energy. *Arch. Rational Mech. Anal.* **100**, 13–52.

J. M. BALL & R. D. JAMES [1990] Proposed experimental tests of a theory of fine microstructure and the two–well problem (*preprint*).

Z. S. BASINSKI & J. W. CHRISTIAN [1954] Experiments on the martensitic transformation in single crystals of indium–thallium alloys. *Acta Metall.* **2**, 148–166.

P. BAUMANN & D. PHILLIPS [1990] A nonconvex variational problem related to change of phase. *Applied Mathematics and Optimization* **21**, 113–138.

C. BENNET & R. SHARPLEY [1988] *Interpolation of Operators.* Academic Press, Boston, San Diego, New York, Berkeley.

K. BHATTACHARYA [1991] Wedge–like microstructures in martensites. *Acta Metall. Mater.* **39**, no. 10, 2431–44.

C. CANUTO, M. Y. HUSSAINI, A. QUARTERONI & T. A. ZANG [1988] *Spectral Methods in Fluid Dynamics.* Springer–Verlag, Heidelberg, Berlin.

M. CHIPOT [1991] Numerical analysis of oscillations in nonconvex problems. *Numer. Math.* **59**, 747–767.

P. G. CIARLET [1988] *Mathematical Elasticity I: Three dimensional Elasticity.* North–Holland.

C. COLLINS & M. LUSKIN [1989] The computation of the austenitic–martensitic phase transition, in *"Partial Differential Equations and Continuum Models of Phase Transitions*, (ed. by M. Rascle, D. Serre, and M. Slemrod). Springer Lecture Notes in Physics 344, 34–50, Springer–Verlag.

C. M. DAFERMOS [1973] The entropy rate admissibility criterion for solutions of hyperbolic conservations laws. *Journal of Differential Equations* **14**, 202–212.

C. M. DAFERMOS [1983] Hyperbolic systems of conservation laws, in *Systems of Nonlinear Partial Differential Equations* (ed. J. M. Ball), D. Reidel, Dordrecht.

H. ENGLER [1989] Global regular solutions for the dynamic antiplane shear problem in nonlinear viscoelasticity. *Math. Zeitschrift* **202**, 251–259.

J. L. ERICKSEN [1975] Equilibrium of bars. *J. Elast.* **5**, 191–201.

J. L. ERICKSEN [1980] Some phase transitions in crystals. *Arch. Rational Mech. Anal.* **73**, 99–124.

L. C. EVANS [1990] *Weak convergence methods for nonlinear partial differential equations.* CBMS Regional Conference Series in Mathematics No. 74, AMS, Providence.

D. A. FRENCH & L. B. WAHLBIN [1991] On the numerical approximation of an evolution problem in nonlinear viscoelasticity. *Mathematical Sciences Institute. Technical Report* 91-49, Cornell University.

E. FRIED [1991] On the construction of two–phase equilibria in a non–elliptic hyperelastic material (*preprint*).

D. FUJIWARA & H. MORIMOTO [1977] An L_r–theorem of the Helmholtz decomposition of vector fields. *J. Fac. Sci. Univ. Tokyo, Sec. I.* **24**, 685–700.

J. W. GIBBS [1876] On the equilibrium of heterogenous substances *Trans. Conn. Acad. vol III*, 108–248, in *The Scientific Papers of J. W. Gibbs, Vol I: Thermodynamics.* Dover, New York, 1961.

P. GRISVARD [1985] *Elliptic Problems in Nonsmooth Domains.* Pitman, Boston.

M. E. GURTIN & A. STRUTHERS [1990] Multiphase thermomechanics with interfacial structure. 3. Evolving phase boundaries in the presence of bulk deformation. *Arch. Rational Mech. Anal.* **112**, 97–160.

M. E. GURTIN & R. TEMAM [1981] On the anti-plane shear problem in finite elasticity. *J. Elast.* **2**, 197–206.

J. K. HALE [1988] *Asymptotic Behavior of Dissipative Systems.* AMS, Providence.

D. HENRY [1981] *Geometric Theory of Semilinear Parabolic Equations.* Springer Lecture Notes in Mathematics No. 840, Springer–Verlag, New York.

P. J. HOLMES & P. J. SWART [1991] A Mathematical cartoon for the dynamics of fine structure. *Transactions of the Eighth Army Conference on Applied Mathematics and Computing*, ARO Report 91–1, 11–21, Ithaca.

T. J. R. HUGHES, T. KATO & J. E. MARSDEN [1977] Well-posed quasi-linear hyperbolic systems with applications to nonlinear elastodynamics and general relativity. *Arch. Rational Mech. Anal.* **63**, 273–304.

R. D. JAMES [1979] Co–existent phases in the one–dimensional static theory of elastic bars. *Arch. Rational Mech. Anal.* **72**, 99–139.

R. D. JAMES [1980] The propagation of phase boundaries in elastic bars. *Arch. Rational Mech. Anal.* **73**, 125–158.

R. D. JAMES [1981] Finite deformations by mechanical twinning. *Arch. Rational Mech. Anal.* **77**, 143–176.

T. KATO [1966] *Perturbation Theory for Linear Operators.* Springer–Verlag, New York.

J. K. KNOWLES [1976] On finite anti-plane shear for incompressible elastic materials. *J. Australian Math. Soc.* **19B**, 400–415.

J. K. KNOWLES [1977] The finite anti-plane shear field near the tip of a crack for a class of incompressible elastic solids. *Int. J. Fracture* **13**, 611–639.

J. K. KNOWLES & E. STERNBERG [1975] On the ellipticity of the equations of nonlinear elastostatics for a special material. *J. Elast.* **5**, 341–361.

J. K. KNOWLES & E. STERNBERG [1977] On the failure of ellipticity of the equations for finite elastostatics plane strain. *Arch. Rational Mech. Anal.* **63**, 221–236.

J. K. KNOWLES & E. STERNBERG [1978] On the failure of ellipticity and the emergence of discontinuous deformation gradients in plane finite elastostatics. *J. Elast.* **8**, 329–379.

J. K. KNOWLES & E. STERNBERG [1980] Discontinuous deformation gradients near the tip of a crack in finite anti-plane shear: an example. *J. Elast.* 10, 81-110.

R. V. KOHN & S. MŰLLER [1992] Branching of twins near an austenite/twinned-martensite interface, (to appear in) *Phil Mag. A.*

S. LARSSON, V. THOMEÉ & L. B. WAHLBIN [1991] Finite-element methods for a strongly damped wave equation. *IMA J. of Numer. Anal* 11, 115-142.

J. P. LASALLE & S. LEFSCHETZ [1961] *Stability by Liapunov's Direct Method with Applications.* Academic Press, New York.

L. J. LEITMAN & G. M. C. FISHER [1973] *The Linear Theory of Viscoelasticity.* Handbuch der Physik (ed. S. Fliigge) VI a/3, 1-123, Springer-Verlag, Berlin and New York.

T. MEIS & U. MARCOWITZ [1981] *Numerical solution of partial differential equations.* Springer-Verlag, New York.

M. MIKLAVČIČ [1985] Stability for semilinear parabolic equations with non-invertible linear operator. *Pacific J. of Math* 118, 199-214.

R. L. PEGO [1987] Phase transitions in one-dimensional nonlinear viscoelasticity: admissibility and stability. *Arch. Rational Mech. Anal* 97, 353-394.

P. ROSAKIS [1992] Compact zones of shear transformation in an anisotropic solid, (to appear in) *J. Mech. Phys. Solids.*

P. RYBKA [1992] Dynamical modeling of phase transitions by means of viscoelasticity in many dimensions, (to appear in) *Proc. Roy. Soc. Edinburgh.*

P. L. SACHDEV [1987] *Nonlinear diffusive waves.* Cambridge University Press, Cambridge.

S. A. SILLING [1988a] Numerical studies of loss of ellipticity near singularities in an elastic material. *J. Elast.* 19, 213-239.

S. A. SILLING [1988b] Consequences of the Maxwell relation for anti–plane shear deformations of an elastic solid. *J. Elast.* **19**, 241–284.

M. SLEMROD [1989] A limiting "viscosity" approach to the Riemann problem for materials exhibiting change of phase. *Arch. Rational Mech. Anal.* **105**, 327–365.

P. J. SWART & P. J. HOLMES [1991] Dynamics of phase transitions in nonlinear viscoelasticity (*video animation*). Cornell National Supercomputer Facility.

L. TARTAR [1983] The compensated compactness method applied to systems of conservation laws, in *Material Instabilities in Continuum Mechanics and Related Mathematical Problems* (ed. J. M. Ball). Oxford University Press, 263–285.

H. TRIEBEL [1978] *Interpolation Theory, Function Spaces, Differential Operators.* North–Holland, Amsterdam, New York, Oxford.

C. TRUESDELL & W. NOLL [1965] *The Non-Linear Field Theories of Mechanics.* Handbuch der Physik (ed. S. Flügge) III/3 Springer–Verlag, Berlin.

G. VAN TENDELOO, J. VAN LANDUYT & S. AMELINCKX [1976] The α–β phase transitions in quartz and $AlPO_4$ as studied by electron microscopy and diffraction. *Phys. Stat. Sol.* **a33**, 723–735.

L. B. WAHLBIN [1991] *Private communication.*

W. L. WOOD [1990] *Practical Time–stepping Schemes.* Claredon Press, Oxford.

W. P. ZIEMER [1989] *Weakly Differentiable Functions.* Springer–Verlag, New York.

Center for Nonlinear Analysis
Department of Mathematics
Carnegie Mellon University
Pittsburgh, PA, 15213

Department of Theoretical and Applied Mechanics and Center for Applied Mathematics
Cornell University
Ithaca, NY, 14853